Manuscript JB00440-22, revised

Gac is a transcriptional repressor of the Lyme disease spirochete's OspC virulence-associated surface protein

Tatiana N. Castro-Padovani [1, §], Timothy C. Saylor[1, §], Olivia T. Husted[1, § ,†], Andrew C. Krusenstjerna[1, §], Nerina Jusufovic[1, §], and Brian Stevenson [1,2, *]

1. Department of Microbiology, Immunology, and Molecular Genetics, University of Kentucky College of Medicine, Lexington, Kentucky

2. Department of Entomology, University of Kentucky College of Agriculture, Food, and Ecology, Lexington, Kentucky

§ T.N. Castro-Padovani, T.C. Saylor, O.T. Husted, A.C. Krusenstjerna, and N. Jusufovic contributed equally to this work, and are to be considered equal co-first authors

* For correspondence:
Brian Stevenson, MS421 Medical Center, Department of Microbiology, Immunology, and Molecular Genetics, University of Kentucky College of Medicine, Lexington, Kentucky, USA, 40536-0298

22 † Current address for O.T. Husted: Venture Laboratories, Lexington, KY

23

Abstract

The OspC outer-surface lipoprotein is essential for the Lyme disease spirochete's initial phase of vertebrate infection. Bacteria within the midguts of unfed ticks do not express OspC, but produce high levels when ticks begin to ingest blood. Lyme disease spirochetes cease production of OspC within 1-2 weeks of vertebrate infection, and bacteria that fail to downregulate OspC are cleared by host antibodies. Thus, tight regulation of OspC levels is critical for survival of Lyme borreliae, and therefore an attractive target for development of novel treatment strategies. Previous studies determined that a DNA region 5′ of the *ospC* promoter, the *ospC* operator, is required for control of OspC production. Hypothesizing that the *ospC* operator may bind a regulatory factor, DNA affinity pulldown was performed, and identified binding by the Gac protein. Gac is encoded by the C-terminal domain of the *gyrA* open reading frame, from an internal promoter, ribosome-binding site, and initiation codon. Our analyses determined that Gac exhibits a greater affinity for *ospC* operator and promoter DNAs than for other tested borrelial sequences. In vitro and in vivo analyses demonstrated that Gac is a transcriptional repressor of *ospC*. These results constitute a substantial advance to our understanding the mechanisms by which the Lyme disease spirochete controls production of OspC.

43 **Importance**

44 *Borrelia burgdorferi* (sensu lato) requires its surface-exposed OspC protein in order to
45 establish infection of humans and other vertebrate hosts. Bacteria that either do not
46 produce OspC during transmission, or fail to repress OspC after infection is established,
47 are rapidly cleared by the host. Herein, we identified a borrelial protein, Gac, that
48 exhibits preferential affinity to the *ospC* promoter and 5′ adjacent DNA. A combination
49 of biochemical analyses and investigations of genetically-manipulated bacteria
50 demonstrated that Gac is a transcriptional repressor of *ospC*. This is a substantial
51 advance toward understanding how the Lyme disease spirochete controls production of
52 the essential OspC virulence factor, and identifies a novel target for preventative and
53 curative therapies.

54

55

56 **Introduction**

57 The Lyme disease spirochete, *Borrelia burgdorferi* sensu lato (*B. burgdorferi* sl),
58 requires its OspC protein during the initial stages of vertebrate infection, and mutant
59 bacteria that cannot produce this outer surface-exposed lipoprotein are unable to
60 initiate infection of vertebrates (1-5). Production of OspC is tightly regulated. *B.*
61 *burgdorferi* sl within the midguts of unfed ticks do not express OspC (6, 7). As ticks
62 begin to feed on host blood, spirochetes initiate production of OspC, with the large
63 majority producing detectable quantities of OspC at the time of transfer from tick to
64 vertebrate (6, 8-11). The essential function(s) of OspC is not conclusively known - it can
65 bind a tick salivary protein and vertebrate plasminogen and complement C4b - but may
66 have additional functions (12-22). Infected humans and other animals mount strong
67 antibody responses against OspC within days of infection (23-26). At the same time, *B.*
68 *burgdorferi* sl represses expression of OspC, and spirochetes that do not shut off OspC
69 synthesis are cleared by immunocompetent hosts (2, 3, 5, 27-31). Thus, regulation of
70 OspC may be an excellent target for novel therapeutics to prevent and/or clear *B.*
71 *burgdorferi* infections.

72 OspC was the first *B. burgdorferi* sl protein to be identified as being regulated
73 during the natural tick-vertebrate infectious cycle (6). As noted above, OspC is not
74 produced in unfed ticks, but is highly expressed in feeding ticks and during the earliest
75 stages of vertebrate infection (6, 8). Regulated production can also be manipulated in
76 culture, with bacteria grown at 23˚C, pH=7.5, or culture media that yield slow
77 replication rates, producing low to no OspC, while the protein is highly expressed

78 following transfer from those conditions to 35˚C, pH=6.5, or complete culture media,
79 respectively (6, 32-34). It is not yet known how those culture conditions are interpreted
80 by *B. burgdorferi* sl to modulate OspC levels, but they provide convenient means to
81 evaluate borrelial regulatory mechanisms.

82 An alternative sigma factor, RpoS, is also affected by the above-described
83 infection and culture conditions (34-37). RpoS controls production of numerous *B.*
84 *burgdorferi* sl proteins that are required for vertebrate infection (36, 38, 39). Deletion of
85 *rpoS* blocks induction of OspC, which has led to a hypothesis that expression of *ospC* is
86 solely due to RpoS-RNA polymerase holoenzyme directly transcribing from the *ospC*
87 promoter (36, 37, 40, 41). Yet, there is evidence that transcriptional control of *ospC* is
88 more complicated than that model assumes. Previous studies found that a region of
89 DNA 5' of the *ospC* transcriptional start site, designated the *ospC* operator, is necessary
90 for induction of *ospC* transcription (42-44).

91 *B. burgdorferi* sl has been divided into several clades that are often referred to as
92 genospecies, which include *B. burgdorferi* sensu stricto (*B. burgdorferi* ss) and *B. garinii*.
93 An earlier study noted that the *ospC* operator of *B. burgdorferi* ss type strain B31 includes
94 a pair of inverted repeat sequences (Fig. 1) (44, 45). Yet, those inverted repeats are found
95 in only a subset of Lyme disease borreliae (46). However, the *ospC* operators of all
96 examined Lyme spirochetes contain two or more copies of a conserved 11bp directly-
97 repeating sequence (Fig. 1 and (46)). *B. burgdorferi* ss B31 contains two copies of the 11bp
98 repeat, which overlap the previously discussed inverted repeats (Fig. 1 and (44, 46)). In
99 contrast, the *ospC* operators of some strains of the *B. garinii* genospecies contain seven

100 adjacent copies of the 11bp repeat (Fig. 1). All *ospC* promoters also contain a copy of the
101 11bp repeat, oriented in the opposite direction (Fig. 1). The retention of the 11bp repeat
102 suggested to us that it may be a key component of *ospC* regulation, with sequence
103 conservation pointing toward it being a binding site for a regulatory protein. To address
104 that hypothesis, we performed DNA-binding studies with borrelial cytoplasmic extract,
105 identified a component protein that has affinity for the *ospC* operator, and identified a
106 functional role for that protein as a transcriptional repressor of *ospC*.

107 **Results**

108 **Identification of Gac as an *ospC* operator-binding protein.** As a first step, an
109 infectious clone of the *B. burgdorferi* ss type strain, B31-MI-16, was cultured to mid-
110 exponential phase at 35˚C. That condition was adopted based on our previous
111 characterization of the *B. burgdorferi erp* operons, whose expression is also responsive to
112 culture temperature, in which we found that the *erp* repressing and activating proteins
113 were all adequately expressed when cultured at 35˚C (47-49).

114 A fluorescently-tagged DNA sequence corresponding to the *ospC* operator region
115 of *B. garinii* Ip89 was incubated with the B31-MI-16 cytoplasmic extract, then subjected
116 to electrophoretic mobility shift electrophoresis (EMSA). The strain Ip89 sequence was
117 used for these analyses under the hypothesis that a protein that binds to the 11bp
118 repeated sequence would have an overall greater affinity for the 7 direct repeats of Ip89
119 as opposed to the smaller number of separated repeats of B31 (Fig. 1). Addition of the
120 cytoplasmic extract resulted in retarded mobility of the labeled DNA probe, indicating
121 that a borrelial component bound to the DNA (Fig. 2A).

122 Ip89 *ospC* operator DNA was again PCR amplified, but with one of the
123 oligonucleotide primers containing a 5′ biotin moiety. That DNA was adhered to
124 streptavidin-coated magnetic beads, incubated with B31 cytoplasmic extract, washed
125 extensively, then bound proteins eluted with buffers having progressively greater
126 concentrations of NaCl. Aliquots of each eluted fraction were subjected to SDS-PAGE
127 and proteins stained with SYPRO-Ruby. A protein band with an approximate molecular
128 mass of 30-35 kDa eluted at 0.3 and 0.5 M NaCl (Fig. 2B). The bands were excised from

129 the gel, subjected to trypsin digestion and mass spectrometry, and results compared to
130 the predicted proteome of strain B31. Only one potential match was obtained, to the
131 GyrA subunit of DNA gyrase, with 9 unique peptides identified. Notably, all of the
132 identified peptide fragments mapped to the C-terminal half of GyrA (Fig. 2C).

133 Bacterial DNA gyrases are comprised of two subunits, GyrA and GyrB (50).
134 GyrA proteins possess a unique C-terminal domain that bends DNA to facilitate the
135 topoisomerase activity of the gyrase (51, 52). Curiously, Lyme disease borreliae produce
136 two separate proteins from the *gyrA* locus, a full length GyrA protein and a second, 35
137 kDa protein named Gac, which is transcribed from an internal promoter and consists
138 solely of the C-terminal DNA-binding domain (52-54) (Fig. 2D, and Fig. S1). We
139 pursued the possibility that Gac preferentially binds to *ospC* operator DNA and thereby
140 affects production of OspC.

141

142 **Gac exhibits affinity for the *ospC* operator and promoter.** To address the
143 question of Gac affinity, labeled DNA probes were constructed that consisted of either
144 the strain Ip89 or B31 *ospC* operators (Fig. 1). Additional unlabeled DNAs were
145 produced for use as EMSA competitors: each of the *ospC* operators, truncated segments
146 of the B31 *ospC* operator, and DNA sequences corresponding to the 5′ ends of the
147 borrelial *flaB* and *ospAB* operons. The Ip89 *ospC* operator probe and competitor were
148 derived by PCR from plasmid pCR2.1 clones, using plasmid-specific M13 Reverse and
149 Forward primers, so an additional unlabeled competitor was produced by PCR of
150 empty pCR2.1, to account for vector-derived DNA sequences.

151 EMSAs of the Ip89 *ospC* operator probe and recombinant Gac found that the
152 protein bound to the labeled probe (Fig 3A, lane 2). Densitometric analyses of EMSAs
153 revealed that Gac exhibits differences in binding affinity to the tested sequences.
154 Addition of 10-times excess of unlabeled Ip89 *ospC* operator resulted in a two-fold
155 reduction in the DNA-Gac EMSA band, while 25-fold excess of unlabeled Ip89 *ospC*
156 operator resulted in greater than an eight-fold reduction in binding and eliminated
157 detectable levels of DNA-protein complexes (Fig. 3A, lanes 3 and 4, respectively).
158 Addition of 25-times excess unlabeled B31 *ospC* operator had little effect on the Ip89
159 operator-Gac complex, indicating a greater affinity of Gac for the Ip89 operator than for
160 the B31 operator (Fig 3A, lane 5). Note that the primary difference between the Ip89 and
161 B31 DNAs is the number of 11bp repeat sequences in their *ospC* operators. Inclusion of
162 25-fold excesses of either empty pCR2.1 amplicon, *flaB*, or *ospAB* unlabeled DNAs also
163 did not compete Gac away from the labeled probe (Fig 3A, lanes 6, 7, and 8,
164 respectively). Thus, Gac displays greater affinity for the Ip89 *ospC* operator than it does
165 for any of the other tested sequences.

166 Similar EMSAs and densitometric analyses were performed with labeled B31
167 *ospC* operator as probe. Unlabeled B31 *ospC* operator DNA effectively competed Gac
168 away from the labeled probe (Fig 3B, lanes 3-4). Addition of a 10-fold excess of
169 unlabeled B31 *ospC* operator competitor was sufficient to reduce binding of Gac by 2.6-
170 fold, while a 25-fold excess of that competitor completely diminished the shift. Inclusion
171 of 10-fold excesses of the empty pCR2.1 amplicon, *flaB*, or *ospAB* unlabeled DNAs
172 exhibited lower levels of competition for Gac binding with none resulting in a fold

173 change of greater than 1.3-times (Fig 3B, lanes 5, 6, and 7, respectively). However, 25-
174 fold excess of each of those unlabeled DNAs competed Gac away from the labeled B31
175 *ospC* labeled probe (Supplemental Figure S1). These results indicate that Gac binds to
176 the B31 *ospC* operator with a greater affinity than to the *flaB, ospAB* or pCR2.1
177 competitor sequences, but has a lower affinity for the B31 *ospC* operator than for the
178 Ip89 *ospC* operator.

179 Using labeled *ospC* operator from strain B31 as the EMSA probe, truncated
180 segments of that DNA region were used as competitors to narrow down the sequences
181 that bound Gac (Fig 4). As above, 10- and 25-fold excesses of unlabeled probe DNA
182 competed Gac away from the B31 *ospC* operator (Fig 4, lanes 3 and 4). No fragment
183 competed as well as the unlabeled probe, although some competed more efficiently
184 than others (Fig. 4, lanes 5-11). Notably, competitor D was more effective that the
185 similarly-sized competitor C, indicating that Gac-binding preferentially involves
186 nucleotides present in competitor D but absent from competitor C. The smaller
187 unlabeled DNAs did not compete as well as the longer DNAs, suggesting that Gac
188 interacts with extended and/or separate sequences in the B31 *ospC* 5′ region. Binding of
189 Gac to DNA has been demonstrated to involve direct interactions with 40-50bp and
190 additional associations with neighboring nucleotides (52, 55-57).

191

192 **Altered *ospC* expression in *gac* mutant *B. burgdorferi*.** To assess the effects of
193 Gac in live *B. burgdorferi*, *gac* mutant strain CKO-1, strain CKO-1(pBLS820) (CKO-1
194 complemented with wild-type *gac*), and strain NGR (an isogenic wild-type *gac* clone)

195 were cultured to mid-exponential phase at 23 ˚C, then diluted into fresh media and
196 incubated to mid-exponential phase at 35 ˚C (6, 32). Immunoblot analyses of lysates of
197 the 23 and 35˚C cultures using OspC-specific antibodies found that all three strains
198 exhibited differential expression of OspC protein, with greater amounts of OspC being
199 synthesized at 35 ˚C (Fig. 5). However, Gac-deficient strain CKO-1 produced 6.4 to 23-
200 times more OspC than did NGR at 23˚C, consistent with Gac being a repressor of OspC
201 synthesis. Levels of OspC in those two strains were very similar at 35˚C, ranging
202 between 0.92 to 1.4 times more OspC in CKO-1 than in NGR. Complementation of
203 CKO-1 with a wild-type *gac* gene on pBLS820 reduced OspC levels by 1.6 to 6.9-times at
204 23˚C, and by 1.2 to 4.3-times at 35˚C. These results suggest that relief of Gac repression
205 is a major contributor to the induction of OspC.

206 *B. burgdorferi* strains NGR and CKO-1 were next transformed with plasmids that
207 carry transcriptional fusions between B31 *ospC* operator/promoter sequences and *gfp*.
208 Plasmid pBLS761 carries the same operator/promoter sequence that was used as the
209 EMSA probe in the above-described studies, while pBLS764 lacks the DNA 5′ of the
210 *ospC* promoter. Each transformant was cultured at 35˚C to mid-exponential phase, then
211 bacterial GFP content was assessed by flow cytometry (Fig. 6). CKO-1(pBLS761)
212 produced substantially greater levels of GFP than did NGR(pBLS761), consistent with
213 the observed levels of OspC protein and transcript described above.

214 NGR(pBLS764), which lacks the *ospC* operator, did not produce GFP (Fig. 6). In
215 contrast, CKO-1(pBLS764) produced GFP at levels comparable to CKO-1(pBLS761). We
216 conclude that absence of Gac relieves transcriptional repression of the *ospC* promoter,

217 and that the *ospC* operator is also required for efficient transcription from the *ospC*
218 promoter if Gac is present. Those results suggest that one or more additional factors
219 interact with *ospC* operator DNA to inhibit Gac binding to the *ospC* promoter. Studies
220 are ongoing to examine that hypothesis.
221
222 ***B. burgdorferi* regulates transcription of *gac*.** Since *ospC* is induced in *B.*
223 *burgdorferi* cultured at 35˚C, we assessed *ospC* and *gyrA/gac* transcript levels over time in
224 cultures of wild-type *B. burgdorferi* (Fig. 7). Levels of *ospC* transcript increased as the
225 cultures grew through exponential into stationary phase. The two *gyrA/gac* primer sets
226 yielded different Q-RT-PCR results for each pair. Since the 5′ primers detected mRNA
227 that only encoded *gyrA*, whereas the 3′ primers detected both *gyrA* and *gac* mRNAs, the
228 relative concentration of *gac* mRNA was approximated by subtracting the results of 5′
229 Q-RT-PCR from results with the 3′ primer set. The concentration of Gac-encoding
230 transcript was greatest during lag and early exponential phases, then declined as the
231 cultures matured and entered stationary phase. Those changes were opposite of *ospC*,
232 and are consistent with the above-described results that indicate Gac is a repressor of
233 *ospC*.
234
235 **Gac exhibits affinity for the telomere of *B. burgdorferi* B31 plasmid lp17.**
236 *Borrelia* species contain both circular and linear DNAs, and there is considerable interest
237 in the mechanisms by which the spirochetes maintain linear replicons (58-60). The Gac
238 protein was initially identified through an affinity pull-down method similar to ours,

239 using a bait sequence derived from a telomere of strain B31's linear plasmid lp17 (53).
240 Having found that Gac preferentially binds to *ospC* 5′ DNAs, we revisited the previous
241 study. A labeled DNA probe with the same telomere-derived sequence was produced,
242 then assessed by EMSA for ability to bind Gac in the presence of excess levels of various
243 unlabeled DNAs. Recombinant Gac produced an EMSA shift with the labeled telomere
244 probe, which was effectively competed away with 10-fold and 25-fold excesses of
245 unlabeled telomere sequence (Fig. 8, lanes 2-4). Ten-fold excesses of unlabeled Ip89 or
246 B31 *ospC* operator DNAs also competed Gac away from the labeled telomere DNA (Fig.
247 8, lanes 6 and 7, respectively). Unlabeled empty pCR2.1 amplicon partly competed for
248 Gac binding, while neither the *flaB* nor the *ospAB* DNAs detectably competed (Fig. 8,
249 lanes 5, 8, and 9, respectively). We conclude that Gac exhibits an affinity for the lp17
250 telomere region that is greater than for the control *ospAB* or *flaB* DNA sequences.
251
252

253 **Discussion**

254 These studies found that Gac exhibits preferential affinity for *ospC* promoter and
255 operator DNA, and inhibits transcription of *ospC*. Studies in wild-type and Gac-
256 deficient mutant bacteria found that absence of Gac resulted in substantially increased
257 expression levels of both native OspC and *ospC* promoter :: *gfp* transcriptional fusions.
258 Those results indicate that Gac is a major contributor to repression of OspC.

259 Deletion of the *ospC* operator did not alleviate Gac-dependent repression of
260 transcription from the *ospC* promoter, suggesting that Gac binding to the promoter itself
261 is sufficient to repress transcription. Additionally, the *ospC* operator is evidently
262 necessary for relief of Gac-dependent transcriptional repression, mirroring results from
263 previous studies that also found that the operator is essential for regulation of *ospC*
264 transcription (42-44). Thus, it appears that one or more unknown factors interact with
265 the *ospC* operator and somehow prevents repression by Gac (Fig. 9). On the hypothesis
266 that Gac in wild-type *B. burgdorferi* cytoplasmic extracts might have outcompeted the
267 predicted "factor X" for binding to the *ospC* operator/promoter probe used in the initial
268 DNA affinity pull-downs, we recently performed similar analyses using extract from
269 Gac-deficient mutant CKO-1. Salt fractionation and SDS-PAGE revealed two proteins
270 with sizes different from Gac (our unpublished results). We are currently examining
271 whether these might be the hypothesized "factor X" anti-repressor.

272 An earlier study found that inhibition of *B. burgdorferi* DNA gyrase function by
273 addition of coumermycin resulted in increased production of OspC protein (44).
274 Considering the effect of Gac on *ospC* expression, it will be important to determine

275 whether the effect of coumermycin is due to changes in DNA topology at the *ospC*
276 operon, changes in levels of Gac or other regulatory proteins, or a combination of those
277 and, perhaps, other factors.

278 Our studies found that Gac has elevated affinity for three sites in the *B.*
279 *burgdorferi* genome – the *ospC* operator, the *ospC* promoter, and the telomere of lp17 –
280 yet can also possesses lesser affinity for other DNA sequences. Gac wraps DNA around
281 itself, forming 180-220˚ bends (52). Gac complements some features of the *E. coli*
282 nucleoid-associate protein HU when expressed in that species (53, 54). Taken together,
283 these data suggest that Gac may be a nucleoid-associated protein ("histone-like
284 protein"). It is not uncommon for nucleoid-associated proteins to also influence
285 transcription (61-63). Indeed, the antirepressor of *B. burgdorferi erp* operon transcription,
286 EbfC, meets the criteria of being an NAP (64).

287 The ability of Gac to preferentially bind to certain DNA sequences raises the
288 possibility that GyrA, alone or as part of DNA gyrase, might also have a preference for
289 these sequences. We are currently investigating this possibility, as it could affect gene
290 expression and aspects of DNA supercoiling .

291 At this time, it is not known whether production of a separate Gac protein from
292 the 3′ end of the *gyrA* ORF is unique to *B. burgdorferi*. The possibility that *gyrA* can
293 encode two distinct proteins has never been addressed for the vast majority of other
294 bacterial species. It would be worth examining other *gyrA* genes for presence of
295 potential ribosome binding sites and start codons near the beginning of the C-terminal
296 domain.

297 In conclusion, our investigations found that *B. burgdorferi* Gac has elevated
298 affinity for *ospC* operator/promoter DNAs. Gac repressed *ospC* transcription in vitro
299 and in live spirochetes. Levels of *ospC* and *gac* transcripts changed in opposite directions
300 during cultivation, consistent with *ospC* repression by Gac. Analyses of mutants
301 indicate that the *ospC* operator is required to alleviate Gac repression of the *ospC*
302 promoter, implying that one or more additional factors interact with the *ospC* operator
303 to prevent repression by Gac. The Gac protein also bound with elevated affinity to an
304 lp17 telomere, suggesting that it might play a role in linear DNA maintenance. Our
305 observations, and those of others (52, 53), indicate that Gac functions like a nucleoid
306 associated protein that exerts effects on gene regulation and genomic structure.

307 **Materials and Methods**

308 **Bacteria, plasmids, and culture conditions.** *B. burgdorferi* sensu stricto strain B31
309 is the type strain, and was isolated from an *Ixodes scapularis* tick that was collected on
310 Shelter Island, New York (65, 66). Infectious clone B31-MI-16 was used to prepare
311 cytoplasmic extracts for identification of *ospC* operator-binding proteins (67). *B. garinii*
312 strain Ip89 was isolated from an *I. persulcatus* tick that was collected in central Eurasia
313 (68, 69).

314 *Borrelia* spp. strains were cultured in BSK-II broth at either 23 or 35˚C (70).
315 Temperature shift cultivation was performed by diluting a 23˚C culture 1:100 into fresh
316 medium, then incubating at 35˚C (32). Culture densities were determined with a Petroff-
317 Hausser counting chamber and dark field microscopy.

318 Analyses of the effects of Gac on OspC expression used a Δ*gac* clone of strain
319 B31, CKO-1, and an isogenic control strain, NGR (54). The overlap of the *gac* ORF with
320 the essential *gyrA* ORF precludes outright deletion of the *gac* locus. For that reason,
321 Knight et al. (54) produced *gac* defective strain CKO-1 by an allelic exchange mutation
322 that changed the two potential *gac* start codons from ATG to CTT and ATT (leucine and
323 isoleucine, respectively) and the ribosome binding site from AGGAGG to AGAAGA.
324 The mutant does not produce a Gac protein, although it does produce normal levels of
325 GyrA (54). The *gac* mutations were selected by simultaneous introduction of point
326 mutations into the adjacent *gyrB* gene, which confer resistance to coumermycin (54, 71).
327 The CKO-1 *gac* mutant exhibits growth patterns that are physiologically

328 indistinguishable from the wild-type parent or from NGR, an isogenic coumermycin-
329 resistant *gyrB* strain (54).

330 Plasmid pBLS820 was custom produced by GenScript (Piscataway, NJ) by
331 cloning the *B. burgdorferi gac* open reading frame, ribosome-binding site, and promoter
332 into vector pBSV2-G (Supplemental Fig. S2) (72). *B. burgdorferi* CKO-1 was transformed
333 by electroporation, and transformants were selected by culture in 150 μg/ml
334 gentamicin.

335 Plasmid pBLS761 contains the B31 *ospC* promoter and operator in a
336 transcriptional fusion with *gfp*. Plasmid pBLS764 is identical to pBLS761 except that it
337 lacks the *ospC* operator. Both are based on pBLS740, which was produced for this work
338 by cloning the *gfp* gene of pBLS590 between the BamHI and HindIII sites of vector
339 pKFSS1 (73, 74). The *ospC*-derived DNAs used to make pBLS761 and pBLS764 were
340 inserted between the KpnI and BamHI sites of pBLS740, custom synthesized by
341 GenScript. *B. burgdorferi* strains NGR and CKO-1 were individually transformed with
342 plasmids pBLS761 and pBLS764, to produce strains NGR(pBLS761), NGR(pBLS764,
343 CKO-1(pBLS761), and CKO-1(pBLS764). Two of our previously-described *B. burgdorferi*
344 strains were used as GFP expression controls: KS10, which carries a promoterless *gfp* on
345 pBLS590, and KS20, which carries the constitutively-expressed minimal *erpAB* promoter
346 driving *gfp* on pBLS599 (73). Plasmids pBLS590 and pBLS599 confer resistance to
347 kanamycin. *B. burgdorferi* containing pBLS590 or pBLS599 were cultured in media that
348 contained 200 μg/ml kanamycin, while spirochetes that contain pBLS761 or pBLS764
349 were cultured in media with 50 μg/ml streptomycin (73-76).

350

351 **Cytoplasmic extracts for EMSA.** *B. burgdorferi* ss B31-MI-16 was cultured at 35˚C
352 to mid-exponential phase (approximately $5x10^7$ bacteria/ml). Bacteria were harvested
353 by centrifugation, washed with phosphate buffered saline (PBS), and resuspended in a
354 minimal volume of 50mM Tris (pH=7.6), 10mM EDTA, 10% (w/vol) sucrose. The
355 suspension was frozen in a dry ice/ ethanol bath, then allowed to thaw in an ice-water
356 bath. NaCl, dithiothreitol, and lysozyme were added to final concentrations of 140 mM,
357 1 mM, and 0.4 mg/ml, respectively, and incubated on ice for 5 min. The cell mixture
358 was subjected to four additional freeze-thaw cycles. Cellular debris was pelleted by
359 centrifugation, and the supernatant was aliquoted and stored at -80˚C (77).

360

361 **Electrophoretic mobility shift assays (EMSAs).** Labeled and unlabeled nucleic
362 acids are described in Supplementary Table 1. Fluorescently tagged IRDye800 labeled
363 probes were utilized for EMSAs. For each EMSA binding reaction, a labeled probe was
364 incubated for 15 min at room temperature with protein and unlabeled competitor DNA
365 as necessary, in EMSA buffer (50mM Tris-HCl, 25mMKCl, 10% glycerol (vol/vol),
366 0.01% Tween 20, 100nM dithiothreitol, and 1mM phenylmethanesulfonyl fluoride
367 (PMSF). Protein-nucleic acid mixtures were then loaded into either 6% or 10% Novex
368 TBE gels (Thermo Fisher). Gels were pre-run for at least 30 min at 100V in 0.5x TBE
369 buffer before sample loading. Following the addition of the samples, electrophoresis
370 was conducted for up to 1.5 h at 100V.

371 Initially, a fragment of *B. garinii* Ip89 DNA, from 5′ of the *ospC* operator through
372 the *ospC* promoter, was amplified from genomic DNA by PCR with oligonucleotide
373 primers 1021 and 1022 (Supplementary Table 1). The resulting amplicon was cloned
374 into pCR2.1 (Invitrogen) to create pBLS756. Fluorescently-tagged IP89 *ospC* operator
375 was produced by PCR of pBLS756 using IRDye800-tagged M13-Reverse and unlabeled
376 M13-Forward primers (Supplementary Table 1). The probe was incubated with cleared
377 borrelial cytoplasmic extract in EMSA buffer for 15 min at room temperature with 10ng
378 poly-dI-dC, then subjected to electrophoresis. These exploratory EMSAs were
379 performed twice.

380 Other EMSAs used purified recombinant Gac protein, labeled *ospC*
381 operator/promoter probes, and unlabeled DNA competitors. Unless noted otherwise,
382 all EMSAs were performed a minimum of three times.

383 In addition, a sub-telomeric sequence of strain B31 lp17 was amplified from total
384 genomic DNA by PCR with oligonucleotides TL16h and TL16g as previously described
385 (53). The resulting PCR product was cloned into pCR2.1 (Invitrogen) and maintained in
386 *E. coli* TOP-10. The amplicon was completely sequenced on both strands to ensure
387 fidelity. Fluorescently tagged telomere probe was produced by PCR using IRDye800
388 tagged M13-Reverse and unlabeled M13-Forward primers.

389 Densitometric analyses of EMSAs was performed using Image Lab 6.1 (Bio-Rad)
390 software. Lanes and bands were added manually and subsequently analyzed to
391 generate the lane percentage totals for each band in a lane. Protein-DNA shifts were
392 considered as the entire region above the free DNA in each lane. The free DNA was

393 determined for each lane by analyzing the band percentage values. For each EMSA, the
394 free DNA percentage values for all lanes were normalized to the probe-only control
395 band percentage value. This set the free DNA percentage of the probe-only control as
396 equal 100%. The normalized free DNA values were then subtracted from 100% to
397 calculate the percent shifted DNA in each lane. Fold changes in DNA binding of EMSA
398 competition assays were calculated by dividing the percent shifted in competition lanes
399 by the percent shifted of the protein-probe only lane.
400
401 **DNA affinity pull-down.** Proteins that bind *ospC* operator DNA were purified
402 from B31-MI-16 cytoplasmic extracts as previously described (78). Briefly, bacteria of a
403 mid-exponential phase (approximately $5x10^7$ bacteria/ml) culture were harvested,
404 washed, and frozen at -80˚C. Bacterial pellets were then thawed on ice, and subjected to
405 three additional rounds of freezing at -80˚C / thawing on ice. Bacterial lysates were
406 resuspended in a minimal volume of BS/THES buffer (44.3% THES buffer, 20% BS
407 buffer, 35.7% water). THES Buffer consists of 50mM Tri HCl (pH 7.5), 10mM EDTA,
408 20% sucrose (w/vol), 140mM NaCl, 0.7% (vol/vol) Protease Inhibitor Cocktail II
409 (Sigma), and 0.1% (vol/vol) Phosphatase Inhibitor Cocktail II (Sigma). BS buffer
410 consists of 50mM HEPES (pH=7.5), 25mM $CaCl_2$, 250mM KCl, and 60% (vol/vol)
411 glycerol. Suspended bacteria were lysed by sonication, on ice. Cellular debris was
412 pelleted by centrifugation, and the supernatant was divided into aliquots.

413 Recombinant plasmid pBLS756, which contains the *B. garinii* Ip89 *ospC*
414 operator/promoter sequence, was used as template to produce a biotin-tagged
415 amplicon by PCR with biotin-tagged M13-Reverse and unlabeled M13-Forward primers
416 (Supplementary Table 1). The probe was incubated with cleared borrelial cytoplasmic
417 extract in EMSA buffer for 15 min at room temperature with 10ng poly-dI-dC, then
418 subjected to electrophoresis. The bait DNA was bound to streptavidin Dynal beads
419 (Invitrogen), then washed with BS/THES buffer. Cytoplasmic extracts were incubated
420 with the DNA-bound beads, and washed extensively with BS/THES. Bound proteins
421 were eluted by washing with buffer containing increasing NaCl concentrations to 0.2,
422 0.3, 0.5, 0.75, and 1.0 M. Fractions were analyzed by SDS-PAGE, and proteins were
423 stained with SYPRO-Ruby (Molecular Probes, Eugene, OR). A protein band that eluted
424 at 0.3 and 0.5 M NaCl was cut out. The samples were treated with trypsin and assayed
425 by LC-MS-MS at the University of Kentucky Proteomics Core. Results were compared
426 with the *B. burgdorferi* strain B31-MI sequence (59, 60) using Mascot (Matrix Science,
427 Boston).
428
429 **Recombinant Gac protein.** The B31 *gac* ORF was cloned into pET101, then
430 sequenced to confirm fidelity. C-terminally His-tagged Gac was expressed in *E. coli*
431 Rosetta II upon induction with 1 mM of isopropyl-β-D-thiogalactopyranoside (IPTG)
432 for 1 hour at 37°C. Bacteria were collected by centrifugation, and the pellet was frozen
433 at -80°C. The bacterial pellet was then thawed on ice, resuspended in phosphate
434 buffered saline (PBS) containing 10 mM imidazole, and bacteria lysed by sonication.

435 The sonicate was subjected to centrifugation, then recombinant protein purified from
436 the soluble fraction using HisPur Ni-NTA columns (Thermo Scientific). Purified
437 proteins were dialyzed against EMSA buffer. Protein concentrations were determined
438 by Bradford assay and purity assessed by SDS-PAGE with Coomassie brilliant blue
439 staining.
440
441 **Immunoblot analyses.** Cultures of strains NGR, CKO-1, and CKO-1(pBLS820)
442 were harvested at mid-exponential phase by centrifugation, then split into aliquots for
443 immunoblot assays and RNA extraction. Pellets for immunoblot assays were frozen at -
444 80°C, subsequently thawed at room temperature, then resuspended in 10% SDS, boiled
445 for 5-minutes, and vigorously vortexed. The resulting lysates were stored at 4°C. Prior
446 to electrophoresis, samples were preheated to 42° before adding to 2x sodium dodecyl
447 sulfate (SDS)-page loading dye (63mM Tris pH7.5, 18.75% [mass/vol] glycerol, 10%
448 [vol/vol] 2-mercaptoethanol, 4% [mass/vol] SDS, and .5% [mass/vol] bromophenol
449 blue). Separation by SDS-polyacrylamide gel electrophoresis was followed by
450 electrotransfer to nitrocellulose membranes and blocking with 5% nonfat dried milk in
451 Tris-buffered saline-Tween-20 (20 mM Tris [pH 7.5], 150 mM NaCl, 0.05% [vol/vol]
452 Tween-20). The membranes were then incubated with murine monoclonal antibodies
453 directed against FlaB or OspC (79, 80). After incubation with primary antibodies,
454 membranes were incubated with goat anti-mouse IgG conjugated to IRDye800 (LI-Cor).
455 Immunoblots were imaged with a ChemiDoc MP (Bio-Rad, CA) and densities analyzed

456 with background compensation using Image-Lab software (Bio-Rad). All immunoblots
457 were performed a minimum of three times.
458
459 **Flow cytometric analysis of GFP expression.** Transcriptional activity of *ospC*
460 promoter::*gfp* reporter constructs was assayed essentially as we previously described
461 (73). Briefly, cultures of s NGR(pBLS761), NGR(pBLS764, CKO-1(pBLS761), CKO-
462 1(pBLS764), KS10, and KS20 were grown to mid-exponential phase (approximately
463 $5x10^7$ bacteria per ml) in BSK-II broth at 35˚C. Bacteria were collected by centrifugation,
464 washed twice with phosphate-buffered saline (PBS), then resuspended in PBS at
465 concentrations of approximately 10^6 bacteria per ml. Aliquots of each bacterial
466 suspension were analyzed using a FACSymphony flow cytometer (Becton Dickinson,
467 San Jose, Calif.), with excitation and detection wavelengths of 488 and 530 nm,
468 respectively. Approximately 100,000 events were measured for each flow cytometry
469 analysis.
470
471 **Quantitative reverse transcription PCR (Q-RT-PCR).** *B. burgdorferi* was cultured
472 at 35ºC, and 2 ml aliquots of bacteria were taken 1-, 3-, 5-, 7-, 9-, and 11-days post-
473 inoculation. Bacteria were pelleted, then washed two times with PBS and frozen at -
474 80ºC. Frozen pellets were later resuspended in 60ºC TRIzol (Thermo Fisher), and RNA
475 was extracted using Qiagen Mini RNA kits. Residual genomic DNA was depleted using
476 on-column Turbo DNase (Thermo Fisher). The quality (RIN > 7) and quantity of the

477 RNA were determined using an Agilent 2100 Bioanalyzer and Agilent 6000 Nano chips.
478 Purified RNA stocks were stored at -80ºC.

479 Complementary DNA (cDNA) for qPCR was produced using the iScript gDNA
480 Clear cDNA synthesis kits (Bio-Rad). The cDNA stocks were diluted 1:100 into
481 nuclease-free water for use as template. Quantitative PCR was carried out using iTaq
482 Universal SYBR Green Supermix (Bio-Rad) and a Bio-Rad CFX96 Touch Real-time PCR
483 thermocycler. For all reactions, cycles involved melting at 95ºC for 10s, annealing at
484 55ºC for 10 s, and extension at 72ºC for 30s. Each run was performed with technical
485 triplicates of each reaction as well as no-template control reactions that lacked template.
486 Melting curves were performed with each run to validate production of specific
487 amplicons. Every reaction was tested with a reverse transcriptase-negative template to
488 validate the absence of contaminating gDNA. Cq values were normalized to *ftsK*, a gene
489 whose expression is stable across different growth phases (81), using the ΔCq method,
490 and fold-difference was determined by the function $2^{-\Delta Cq}$ (82).

Acknowledgements

This work was funded by NIH grant 3R01AI144126-03S1. We thank Jessamyn Moore for technical assistance and constructive comments; Scott Samuels for providing *B. burgdorferi* strains NGR and CKO-1, and for helpful comments on these studies; Haining Zhu and Jing Chen for assistance with mass spectrometric analyses; and Jennifer Strange, Greg Bowman, and Cuiping Zhang for flow cytometry analyses. Figure 9 was produced using BioRender.com.

501 **References**

502 1. Grimm D, Tilly K, Byram R, Stewart PE, Krum JG, Bueschel DM, Schwan TG,
503 Policastro PF, Elias AF, Rosa PA. 2004. Outer-surface protein C of the Lyme
504 disease spirochete: a protein induced in ticks for infection of mammals. Proc Natl
505 Acad Sci USA 101:3142-3147.

506 2. Stewart PE, Wang X, Bueschel DM, Clifton DR, Grimm D, Tilly K, Carroll JA,
507 Weis JJ, Rosa PA. 2006. Delineating the requirement for the *Borrelia burgdorferi*
508 virulence factor OspC in the mammalian host. Infect Immun 74:3547-3553.

509 3. Tilly K, Krum JG, Bestor A, Jewett MW, Grimm D, Bueschel D, Byram R,
510 Dorward D, Vanraden MJ, Stewart P, Rosa P. 2006. *Borrelia burgdorferi* OspC
511 protein is required exclusively in a crucial early stage of mammalian infection.
512 Infect Immun 74:3554-3564.

513 4. Tilly K, Bestor A, Jewett MW, Rosa P. 2007. Rapid clearance of Lyme disease
514 spirochetes lacking OspC from skin. Infect Immun 75:1517-1519.

515 5. Tilly K, Bestor A, Rosa PA. 2013. Lipoprotein succession in *Borrelia burgdorferi*:
516 similar but distinct roles for OspC and VlsE at different stages of mammalian
517 infection. Mol Microbiol 89:216-227.

518 6. Schwan TG, Piesman J, Golde WT, Dolan MC, Rosa PA. 1995. Induction of an
519 outer surface protein on *Borrelia burgdorferi* during tick feeding. Proc Natl Acad
520 Sci USA 92:2909-2913.

521 7. Fingerle V, Hauser U, Liegl G, Petko B, Preac-Mursic V, Wilske B. 1995.
522 Expression of outer surface proteins A and C of *Borrelia burgdorferi* in *Ixodes*
523 *ricinus*. J Clin Microbiol 33:1867-1869.

524 8. Schwan TG, Piesman J. 2000. Temporal changes in outer surface proteins A and
525 C of the Lyme disease-associated spirochete, *Borrelia burgdorferi*, during the chain
526 of infection in ticks and mice. J Clin Microbiol 38:382-388.

527 9. Pal U, Yang X, Chen M, Bockenstedt LK, Anderson JF, Flavell RA, Norgard MV,
528 Fikrig E. 2004. OspC facilitates *Borrelia burgdorferi* invasion of *Ixodes scapularis*
529 salivary glands. J Clin Invest 113:220-230.

530 10. Skare JT, Shaw DK, Trzeciakowski JP, Hyde JA. 2016. In vivo imaging
531 demonstrates that *Borrelia burgdorferi ospC* is uniquely expressed temporally and
532 spatially throughout experimental infection. PLoS ONE 11:e0162501.

533 11. Fingerle V, Goettner G, Gern L, Wilske B, Schulte-Spechtel U. 2007.
534 Complementation of a *Borrelia afzelii* OspC mutant highlights the crucial role of
535 OspC for dissemination of *Borrelia afzelii* in *Ixodes ricinus*. Int J Med Microbiol
536 297:97-107.

537 12. Ramamoorthi N, Narasimhan S, Pal U, Bao F, Yang XF, Fish D, Anguita J,
538 Norgard MV, Kantor FS, Anderson JF, Koski RA, Fikrig E. 2005. The Lyme
539 disease agent exploits a tick protein to infect the mammalian host. Nature
540 436:573-577.

541 13. Lagal V, Portnoï D, Faure G, Postic D, Baranton G. 2006. *Borrelia burgdorferi* sensu
542 stricto invasiveness is correlated with OspC-plasminogen affinity. Microbes
543 Infect 8:645-652.

544 14. Xu Q, McShan K, Liang FT. 2008. Essential protective role attributed to the
545 surface lipoproteins of *Borrelia burgdorferi* against innate defences. Mol Microbiol
546 69:15-29.

547 15. Earnhart CG, Leblanc DV, Alix KE, Desrosiers DC, Radolf JD, Marconi RT. 2010.
548 Identification of residues within ligand-binding domain 1 (LBD1) of the *Borrelia*
549 *burgdorferi* OspC protein required for function in the mammalian environment.
550 Mol Microbiol 76:393-408.

551 16. Antonara S, Ristow P, McCarthy J, Coburn J. 2010. Effect of *Borrelia burgdorferi*
552 OspC at the site of inoculation in mouse skin. Infect Immun 78:4723-4733.

553 17. Önder Ö, Humphrey PT, McOmber B, Korobova F, Francella N, Greenbaum DC,
554 Brisson D. 2012. OspC is potent plasminogen receptor on surface of *Borrelia*
555 *burgdorferi*. J Biol Chem 287:16860-16868.

556 18. Caine JA, Coburn J. 2015. A short-term *Borrelia burgdorferi* infection model
557 identifies tissue tropisms and bloodstream survival conferred by adhesion
558 proteins. Infect Immun 83:3184-3194.

559 19. Carrasco SE, Troxell B, Yang Y, Brandt SL, Li H, Sandusky GE, Condon KW,
560 Serezani CH, Yang XF. 2015. Outer surface protein OspC is an antiphagocytic
561 factor that protects *Borrelia burgdorferi* from phagocytosis by macrophages. Infect
562 Immun 83:4848-4860.

563 20. Caine JA, Lin YP, Kessler JR, Sato H, Leong JM, Coburn J. 2017. *Borrelia*
564 *burgdorferi* outer surface protein C (OspC) binds complement component C4b
565 and confers bloodstream survival. Cell Microbiol 19:10.1111/cmi.12786.

566 21. Bierwagen P, Szpotkowski K, Jaskolski M, Urbanowicz A. 2019. *Borrelia* outer
567 surface protein C is capable of human fibrinogen binding. FEBS J 286:2415-2428.

568 22. Lin YP, Tan X, Caine JA, Castellanos M, Chaconas G, Coburn J, Leong JM. 2020.
569 Strain-specific joint invasion and colonization by Lyme disease spirochetes is
570 promoted by outer surface protein C. PLoS Pathog 16:e1008516.

571 23. Fuchs R, Jauris S, Lottspeich F, Preac-Mursic V, Wilske B, Soutschek E. 1992.
572 Molecular analysis and expression of a *Borrelia burgdorferi* gene encoding a 22kDa
573 protein (pC) in *Escherichia coli*. Mol Microbiol 6:503-509.

574 24. Fung BP, McHugh GL, Leong JM, Steere AC. 1994. Humoral immune response to
575 outer surface protein C of *Borrelia burgdorferi* in Lyme disease: role of the
576 immunoglobulin M response in the serodiagnosis of early infection. Infect
577 Immun 62:3213-3221.

578 25. Padula SJ, Dias F, Sampieri A, Craven RB, Ryan RW. 1994. Use of recombinant
579 OspC from *Borrelia burgdorferi* for serodiagnosis of early Lyme disease. J Clin
580 Microbiol 32:1733-1738.

581 26. Gilmore RD, Kappel KJ, Dolan MC, Burkot TR, Johnson BJB. 1996. Outer surface
582 protein C (OspC), but not P39, is a protective immunogen against a tick-
583 transmitted *Borrelia burgdorferi* challenge: evidence for a conformational
584 protective epitope in OspC. Infect Immun 64:2234-2239.

585 27. Liang FT, Jacobs MB, Bowers LC, Philipp MT. 2002. An immune evasion
586 mechanism for spirochetal persistence in Lyme borreliosis. J Exp Med 195:415-
587 422.

588 28. Crother TR, Champion CI, Whitelegge JP, Aguilera R, Wu XY, Blanco DR, Miller
589 JN, Lovett MA. 2004. Temporal analysis of the antigenic composition of *Borrelia*
590 *burgdorferi* during infection in rabbit skin. Infect Immun 72:5063-5072.

591 29. Liang FT, Yan J, Mbow ML, Sviat SL, Gilmore RD, Mamula M, Fikrig E. 2004.
592 *Borrelia burgdorferi* changes its surface antigenic expression in response to host
593 immune reponses. Infect Immun 72:5759-5767.

594 30. Xu Q, Seemanapalli SV, McShan K, Liang FT. 2006. Constitutive expression of
595 outer surface protein C diminishes the ability of *Borrelia burgdorferi* to evade
596 specific humoral immunity. Infect Immun 74:5177-5184.

597 31. Tilly K, Bestor A, Dulebohn DP, Rosa PA. 2009. OspC-independent infection and
598 dissemination by host-adapted *Borrelia burgdorferi*. Infect Immun 77:2672-2682.

599 32. Stevenson B, Schwan TG, Rosa PA. 1995. Temperature-related differential
600 expression of antigens in the Lyme disease spirochete, *Borrelia burgdorferi*. Infect
601 Immun 63:4535-4539.

602 33. Carroll JA, Garon CF, Schwan TG. 1999. Effects of environmental pH on
603 membrane proteins in *Borrelia burgdorferi*. Infect Immun 67:3181-3187.

604 34. Jutras BL, Chenail AM, Stevenson B. 2013. Changes in bacterial growth rate
605 govern expression of the *Borrelia burgdorferi* OspC and Erp infection-associated
606 surface proteins. J Bacteriol 195:757-764.

607 35. Yang X, Goldberg MS, Popova TG, Schoeler GB, Wikel SK, Hagman KE, Norgard
608 MV. 2000. Interdependence of environmental factors influencing reciprocal

609 patterns of gene expression in virulent *Borrelia burgdorferi*. Mol Microbiol 37:1470-
610 1479.

611 36. Hübner A, Yang X, Nolen DM, Popova TG, Cabello PC, Norgard MV. 2001.
612 Expression of *Borrelia burgdorferi* OspC and DbpA is controlled by a RpoN-RpoS
613 regulatory pathway. Proc Natl Acad Sci USA 98:12724-12729.

614 37. Caimano MJ, Groshong AM, Belperron A, Mao J, Hawley KL, Luthra A, Graham
615 DE, Earnhart CG, Marconi RT, Bockenstedt LK, Blevins JS, Radolf JD. 2019. The
616 RpoS gatekeeper in *Borrelia burgdorferi*: an invariant regulatory scheme that
617 promotes spirochete persistence in reservoir hosts and niche diversity. Front
618 Microbiol 10:1923.

619 38. Burtnick MN, Downey JS, Brett PJ, Boylan JA, Frye JG, Hoover TR, Gherardini
620 FC. 2007. Insights into the complex regulation of *rpoS* in *Borrelia burgdorferi*. Mol
621 Microbiol 65:277-293.

622 39. Caimano MJ, Iyer R, Eggers CH, Gonzalez C, Morton EA, Gilbert MA, Schwartz
623 I, Radolf JD. 2007. Analysis of the RpoS regulon in *Borrelia burgdorferi* in response
624 to mammalian host signals provides insight into RpoS function during the
625 enzootic cycle. Mol Microbiol 65:1193-1217.

626 40. Eggers CH, Caimano MJ, Radolf JD. 2004. Analysis of promoter elements
627 involved in the transcription initiation of RpoS-dependent *Borrelia burgdorferi*
628 genes. J Bacteriol 186:7390-7402.

629 41. Yang XF, Lybecker MC, Pal U, Alani SM, Blevins J, Revel AT, Samuels DS,
630 Norgard MV. 2005. Analysis of the *ospC* regulatory element controlled by the
631 RpoN-RpoS regulatory pathway in *Borrelia burgdorferi*. J Bacteriol 187:4822-4829.

632 42. Xu Q, McShan K, Liang FT. 2007. Identification of an *ospC* operator critical for
633 immune evasion of *Borrelia burgdorferi*. Mol Microbiol 64:220-231.

634 43. Xu Q, McShan K, Liang FT. 2008. Verification and dissection of the *ospC* operator
635 by using *flaB* promoter as a reporter in *Borrelia burgdorferi*. Microb Pathog 45:70-
636 78.

637 44. Drecktrah D, Hall LS, Hoon-Hanks LL, Samuels DS. 2013. An inverted repeat in
638 the ospC operator is required for induction in *Borrelia burgdorferi*. PLoS One
639 8:e68799.

640 45. Alverson J, Bundle SF, Sohasky CD, Lybecker MC, Samuels DS. 2003.
641 Transcriptional regulation of the *ospAB* and *ospC* promoters of *Borrelia burgdorferi*.
642 Mol Microbiol 48:1665-1677.

643 46. Tilly K, Casjens S, Stevenson B, Bono JL, Samuels DS, Hogan D, Rosa P. 1997. The
644 *Borrelia burgdorferi* circular plasmid cp26: conservation of plasmid structure and
645 targeted inactivation of the *ospC* gene. Mol Microbiol 25:361-373.

646 47. Babb K, Bykowski T, Riley SP, Miller MC, DeMoll E, Stevenson B. 2006. *Borrelia*
647 *burgdorferi* EbfC, a novel, chromosomally-encoded protein, binds specific DNA
648 sequences adjacent to *erp* loci on the spirochete's resident cp32 prophages. J
649 Bacteriol 188:4331-4339.

650 48. Burns LH, Adams CA, Riley SP, Jutras BL, Bowman A, Chenail AM, Cooley AE,
651 Haselhorst LA, Moore AM, Babb K, Fried MG, Stevenson B. 2010. BpaB, a novel
652 protein encoded by the Lyme disease spirochete's cp32 prophages, binds to *erp*
653 Operator 2 DNA. Nucleic Acids Res 38:5443-5455.

654 49. Jutras BL, Chenail AM, Carroll DW, Miller MC, Zhu H, Bowman A, Stevenson B.
655 2013. Bpur, the Lyme disease spirochete's PUR-domain protein: identification as
656 a transcriptional modulator and characterization of nucleic acid interactions. J
657 Biol Chem 288:26220-26234.

658 50. Sugino A, Higgins NO, Cozzarelli NR. 1980. DNA gyrase subunit stoichiometry
659 and the covalent attachment of subunit A to DNA during DNA cleavage. Nucleic
660 Acids Res 8:3865-3874.

661 51. Reece RJ, Maxwell A. 1991. The C-terminal domain of the *Escherichia coli* DNA
662 gyrase A subunit is a DNA-binding protein. Nucleic Acids Res 19:1399-1405.

663 52. Corbett KD, Shultzaberger RK, Berger JM. 2004. The C-terminal domain of DNA
664 gyrase A adopts a DNA-bending beta-pinwheel fold. Proc Natl Acad Sci USA
665 101:7293-7298.

666 53. Knight SW, Samuels DS. 1999. Natural synthesis of a DNA-binding protein from
667 the C-terminal domain of DNA gyrase A in *Borrelia burgdorferi*. EMBO J 18:4875-
668 4881.

669 54. Knight SW, Kimmel BJ, Eggers CH, Samuels DS. 2000. Disruption of the *Borrelia*
670 *burgdorferi gac* gene, encoding the naturally synthesized GyrA C-terminal
671 domain. J Bacteriol 182:2048-2051.

672 55. Liu LF, Wang JC. 1978. DNA-DNA gyrase complex: the wrapping of the DNA
673 duplex outside the enzyme. Cell 15:979-984.

674 56. Fisher LM, Mizuuchi K, O'Dea MH, Ohmori H, Gellert M. 1981. Site-specific
675 interaction of DNA gyrase with DNA. Proc Natl Acad Sci 78:4165–4169.

676 57. Kirkegaard K, Wang JC. 1981. Mapping the topography of DNA wrapped
677 around gyrase by nucleolytic and chemical probing of complexes of unique DNA
678 sequences. Cell 23:721-729.

679 58. Barbour AG, Garon CF. 1987. Linear plasmids of the bacterium *Borrelia*
680 *burgdorferi* have covalently closed ends. Science 237:409-411.

681 59. Fraser CM, Casjens S, Huang WM, Sutton GG, Clayton R, Lathigra R, White O,
682 Ketchum KA, Dodson R, Hickey EK, Gwinn M, Dougherty B, Tomb J-F,
683 Fleischmann RD, Richardson D, Peterson J, Kerlavage AR, Quackenbush J,
684 Salzberg S, Hanson M, van Vugt R, Palmer N, Adams MD, Gocayne J,
685 Weidmann J, Utterback T, Watthey L, McDonald L, Artiach P, Bowman C,
686 Garland S, Fujii C, Cotton MD, Horst K, Roberts K, Hatch B, Smith HO, Venter
687 JC. 1997. Genomic sequence of a Lyme disease spirochaete, *Borrelia burgdorferi*.
688 Nature 390:580-586.

689 60. Casjens S, Palmer N, van Vugt R, Huang WM, Stevenson B, Rosa P, Lathigra R,
690 Sutton G, Peterson J, Dodson RJ, Haft D, Hickey E, Gwinn M, White O, Fraser C.
691 2000. A bacterial genome in flux: the twelve linear and nine circular
692 extrachromosomal DNAs of an infectious isolate of the Lyme disease spirochete
693 *Borrelia burgdorferi*. Mol Microbiol 35:490-516.

694 61. Dorman CJ, Schumacher MA, Bush MJ, Brennan RG, Buttner MJ. 2020. When is a
695 transcription factor a NAP? Curr Opin Microbiol 55:26-33.

696 62. Amemiya HM, Schroeder J, Freddolino PL. 2021. Nucleoid-associated proteins
697 shape chromatin structure and transcriptional regulation across the bacterial
698 kingdom. Transcription 12:182-218.

699 63. Muskhelishvili G, Sobetzko P, Mehandziska S, Travers A. 2021. Composition of
700 transcription machinery and its crosstalk with nucleoid-associated proteins and
701 global transcription factors. Biomolecules 11:924.

702 64. Jutras BL, Bowman A, Brissette CA, Adams CA, Verma A, Chenail AM,
703 Stevenson B. 2012. EbfC (YbaB) is a new type of bacterial nucleoid-associated
704 protein, and a global regulator of gene expression in the Lyme disease
705 spirochete. J Bacteriol 194:3395-3406.

706 65. Burgdorfer W, Barbour AG, Hayes SF, Benach JL, Grunwaldt E, Davis JP. 1982.
707 Lyme disease - a tick-borne spirochetosis? Science 216:1317-1319.

708 66. Johnson RC, Schmid GP, Hyde FW, Steigerwalt AG, Brenner DJ. 1984. *Borrelia*
709 *burgdorferi* sp. nov.: etiologic agent of Lyme disease. Int J Syst Bacteriol 34:496-
710 497.

711 67. Miller JC, von Lackum K, Babb K, McAlister JD, Stevenson B. 2003. Temporal
712 analysis of *Borrelia burgdorferi* Erp protein expression throughout the mammal-
713 tick infectious cycle. Infect Immun 71:6943-6952.

714 68. Xu Y, Johnson RC. 1995. Analysis and comparison of plasmid profiles of *Borrelia*
715 *burgdorferi* sensu lato strains. J Clin Microbiol 33:2679-2685.

716 69. Kraiczy P, Seling A, Brissette CA, Rossmann E, Hunfeld K-P, Bykowski T, Burns
717 LH, Troese MJ, Cooley AE, Miller JC, Brade V, Wallich R, Casjens S, Stevenson B.
718 2008. *Borrelia burgdorferi* complement regulator-acquiring surface protein 2
719 (CspZ) as a serological marker of human Lyme disease. Clin Vaccine Immunol
720 15:484-491.

721 70. Zückert WR. 2007. Laboratory maintenance of *Borrelia burgdorferi*. Curr Protoc
722 Microbiol 12C:1-10.

723 71. Samuels DS, Mach KE, Garon CF. 1994. Genetic transformation of the Lyme
724 disease agent *Borrelia burgdorferi* with coumarin-resistant *gyrB*. J Bacteriol
725 176:6045-6049.

726 72. Elias AF, Bono JL, Kupko JJ, Stewart PE, Krum JG, Rosa PA. 2003. New antibiotic
727 resistance cassettes suitable for genetic studies in *Borrelia burgdorferi*. J Mol
728 Microbiol Biotechnol 6:29-40.

729 73. Babb K, McAlister JD, Miller JC, Stevenson B. 2004. Molecular characterization of
730 *Borrelia burgdorferi erp* promoter/operator elements. J Bacteriol 186:2745-2756.

731 74. Frank KL, Bundle SF, Kresge ME, Eggers CE, Samuels DS. 2003. *aadA* confers
732 streptomycin resistance in *Borrelia burgdorferi*. J Bacteriol 185:6723-6727.

733 75. Bono JL, Elias AF, Kupko JJ, Stevenson B, Tilly K, Rosa P. 2000. Efficient targeted
734 mutagenesis in *Borrelia burgdorferi*. J Bacteriol 182:2445-2452.

735 76. Stewart PE, Thalken R, Bono JL, Rosa P. 2001. Isolation of a circular plasmid
736 region sufficient for autonomous replication and transformation of infectious
737 *Borrelia burgdorferi*. Mol Microbiol 39:714-721.

738 77. Babb K, El-Hage N, Miller JC, Carroll JA, Stevenson B. 2001. Distinct regulatory
739 pathways control the synthesis of *Borrelia burgdorferi* infection-associated OspC
740 and Erp surface proteins. Infect Immun 69:4146-4153.

741 78. Jutras BL, Verma A, Stevenson B. 2012. Identification of novel DNA-binding
742 proteins using DNA-affinity chromatography/pull down. Curr Protocols
743 Microbiol 1F:1-13.

744 79. Barbour AG, Hayes SF, Heiland RA, Schrumpf ME, Tessier SL. 1986. A *Borrelia*-
745 specific monoclonal antibody binds to a flagellar epitope. Infect Immun 52:549-
746 554.

747 80. Mbow ML, Gilmore RD, Stevenson B, Golde WT, Piesman J, Johnson BJB. 2002.
748 *Borrelia burgdorferi*-specific monoclonal antibodies derived from mice primed

749 with Lyme disease spirochete-infected *Ixodes scapularis* ticks. Hybrid
750 Hybridomics 21:179-182.

751 81. Arnold WK, Savage CR, Brissette CA, Seshu J, Livny J, Stevenson B. 2016. RNA-
752 Seq of *Borrelia burgdorferi* in multiple phases of growth reveals insights into the
753 dynamics of gene expression, transcriptome architecture, and noncoding RNAs
754 PLoS One 11:e0164165.

755 82. Krusenstjerna AC, Saylor TC, Arnold WK, Tucker JS, Stevenson B. 2023. *Borrelia*
756 *burgdorferi* DnaA and the nucleoid-associated protein EbfC coordinate expression
757 of the *dnaX-ebfC* operon. J Bacteriol 205: in press.

758 83. Hearnshaw SJ, Edwards MJ, Stevenson CE, Lawson DM, Maxwell A. 2014. A
759 new crystal structure of the bifunctional antibiotic simocyclinone D8 bound to
760 DNA gyrase gives fresh insight into the mechanism of inhibition. J Mol Biol
761 426:2023-2033.

762

763 **Figure Legends**

764

765 **Figure 1.** DNA sequences 5′ of the *ospC* open reading frames of *B. burgdorferi* ss B31 and
766 *B. garinii* Ip89 contain conserved and non-conserved repeated sequences. **(A)** Graphic
767 representation of the 11bp direct repeats (blue arrows) and a distinct, longer inverted
768 repeat sequence in the operator of strain B31 (red arrows), that is not found in strain
769 Ip89 or many other Lyme disease borreliae (44, 46). **(B)** Alignment of the *ospC* 5′ DNA
770 sequences. Strain B31 contains two 11bp repeats that are separated by a unique 8bp
771 sequence, while Ip89 carries seven directly repeated copies. In addition, both strains
772 contain an inverted copy of the 11bp sequence between their -35 and -10 promoter
773 elements.

774

775 **Figure 2. (A)** Electrophoretic mobility shift assay (EMSA) of labeled Ip89 *ospC* operator,
776 without (-) and with (+) cytoplasmic extract from strain B31. The asterisk indicates
777 shifted probe that was present only when borrelial extract was included, indicating
778 presence of a DNA-binding component. Unbound DNA is indicated by "free". Some
779 labeled DNA probe remained in the wells of the gel. **(B)** Cytoplasmic extract from strain
780 B31 was incubated with Ip89 *ospC* operator DNA affixed to beads, eluted with
781 increasing concentrations of NaCl, and eluates were separated by SDS-polyacrylamide
782 gel electrophoresis. Lanes are labeled with the concentration of NaCl used for that
783 elution. The arrow indicated a protein band of 30-35 kDa that eluted in the 0.3 and 0.5
784 mM NaCl washes. **(C)** Amino acid sequence of GyrA and Gac (the two potential

785 initiation methionines of Gac are indicated by boldface and underlining). Mass
786 spectrometry identified nine unique peptides that all mapped to the Gac ORF. Peptides
787 identified with high confidence are shaded green, and those with lower confidence in
788 red. **(D)** Predicted structures of *B. burgdorferi* Gac and GyrA proteins, as determined by
789 AlphaFold (https://alphafold.ebi.ac.uk). Both are consistent with the solved structures
790 of *B. burgdorferi* Gac (52) and the N-terminal domain of *E. coli* GyrA
791 (https://www.rcsb.org/structure/4CKK) (83).
792
793 **Figure 3.** Representative EMSAs of purified recombinant Gac with labeled *ospC*
794 operator/promoter DNAs and unlabeled competitors. Shifted DNAs are indicated with
795 asterisks. Unoccupied DNAs are labeled "free". **(A)** Labeled Ip89 operator/promoter
796 (10 nM) without (lane 1) and with 25 nM Gac (lanes 2-8). Lane 2: no added competitor.
797 Lane 3: plus 10x excess unlabeled Ip89 *ospC* operator/promoter. Lane 4: plus 25x excess
798 unlabeled Ip89 *ospC* operator/promoter. Lane 5: plus 25x excess unlabeled B31 *ospC*
799 operator/promoter. Lane 6: plus 25x unlabeled pCR2.1 amplicon. Lane 7: plus 25x
800 excess unlabeled *flaB* DNA. Lane 8: plus 25x unlabeled *ospAB* DNA. **(B)** Labeled B31
801 operator/promoter (10 nM) without (lane 1) and with 25 nM Gac (lanes 2-7). Lane 2: no
802 added competitor. Lane 3: plus 10x excess unlabeled B31 *ospC* operator/promoter. Lane
803 4: plus 25x excess unlabeled B31 *ospC* operator/promoter. Lane 5: plus 10x unlabeled
804 pCR2.1 amplicon. Lane 6: plus 10x excess unlabeled *flaB* DNA. Lane 7: plus 10x
805 unlabeled *ospAB* DNA.
806

807 **Figure 4.** Mapping Gac binding sites in B31 *ospC* 5′ DNA by EMSA with purified
808 recombinant Gac and unlabeled competitor DNA fragments. Sequences of the probe
809 and competitors are shown above the EMSA, with the 11bp repeats indicated by blue
810 arrows. Shifted DNAs are indicated with asterisks. Unoccupied DNAs are labeled
811 "free". Labeled B31 operator (10 nM) without (lane 1) and with 25 nM Gac (lanes 2-11).
812 Lane 2: no added competitor. Lane 3: plus 10x excess unlabeled B31 *ospC* operator
813 probe. Lane 4: plus 25x excess unlabeled B31 *ospC* operator probe. Lanes 5-11: plus 10x
814 unlabeled competitors A through G, respectively.

815

816 **Figure 5.** Triplicate western blot analyses of strains NGR, CKO-1, and CKO-1(pBLS820)
817 that were cultured to mid-exponential phase at 23 or 35˚C, probed with monospecific
818 antibodies against OspC and FlaB. Results of densitometric analyses are shown in
819 Supplemental Table S2.

820

821 **Figure 6.** Flow cytometric analyses of green fluorescent protein (GFP) levels. Each panel
822 represent approximately 100,000 bacteria that were cultured to mid-exponential phase
823 (approximately $5x10^7$ bacteria/ml) at 35˚C. Isogenic NGR and *gac* mutant CKO-1
824 contained transcriptional fusions of the *ospC* promoter, with an without the operator
825 (pBLS761 and pBLS764, respectively), fused to *gfp*. Negative control strain KS10 carries
826 promoterless *gfp* on pBLS590, and positive control strain KS20 carries the constitutive
827 *erpAB* promoter fused to *gfp* on pBLS599 (73).

828

829 **Figure 7.** Growth curves and quantitative-RT-PCR analyses of selected transcripts of *B.*
830 *burgdorferi* B31, cultured at 35˚C. Bacterial cell densities are indicated by black squares
831 and lines. Relative transcript levels are indicated by red circles and lines. **(A)** Schematic
832 of the locations of amplicons used to determine relative expression of the 5' and 3'
833 portions of *gyrA*. The 5' primer pair amplified only transcripts arising from the
834 promoter 5' of *gyrB*, while the 3' primer pair amplified transcripts arising from both the
835 promoter 5' of *gyrB* and within the *gyrA* ORF. **(B)** Results from the 5′ segment of *gyrA*.
836 **(C)** Results from the 3′ segment of *gyrA*. **(D)** Results from the *gyrA* 3′ segment minus the
837 *gyrA* 5′. **(E)** Analyses of *ospC* transcript levels.

838

839 **Figure 8.** Representative EMSAs of purified recombinant Gac with labeled *ospC* lp17
840 telomere DNA and competitors. Shifted DNAs are indicated with asterisks. Unoccupied
841 DNA is labeled "free". All lanes contain 10 nM labeled lp17 telomere probe, without
842 (lane 1) or with 25 nM Gac (lanes 2-9). Lane 2: no added competitor. Lane 3: plus 10x
843 excess unlabeled lp17 telomere. Lane 4: plus 25x excess unlabeled lp17 telomere. Lane 5:
844 plus 10x unlabeled pCR2.1 amplicon. Lane 6: plus 10x excess unlabeled Ip89 *ospC*
845 operator. Lane 7: plus 10x excess unlabeled B31 *ospC* operator. Lane 8: plus 10x excess
846 unlabeled *flaB* DNA. Lane 9: plus 10x unlabeled *ospAB* DNA.

847

848 **Figure 9.** Graphic summary of these results. Gac binds at or near the 11bp repeated
849 sequences in the *ospC* promoter and operator, and inhibits transcription from the *ospC*

850 promoter. Deletion of the *ospC* operator resulted in ablation of transcription from the
851 *ospC* promoter, as has also been noted previously (42-44). Those data indicate that
852 another factor, "X", interacts with the *ospC* operator and is required to activate
853 transcription. In the absence of Gac, the *ospC* promoter is transcribed at high levels,
854 indicating that "X" competes against Gac repression. X may be one or more protein or
855 other factor. The 11bp repeat sequences are indicated by blue arrows beneath the DNA.
856 The *ospC* promoter -10 and -35 sequences are indicated by black bars above the DNA.

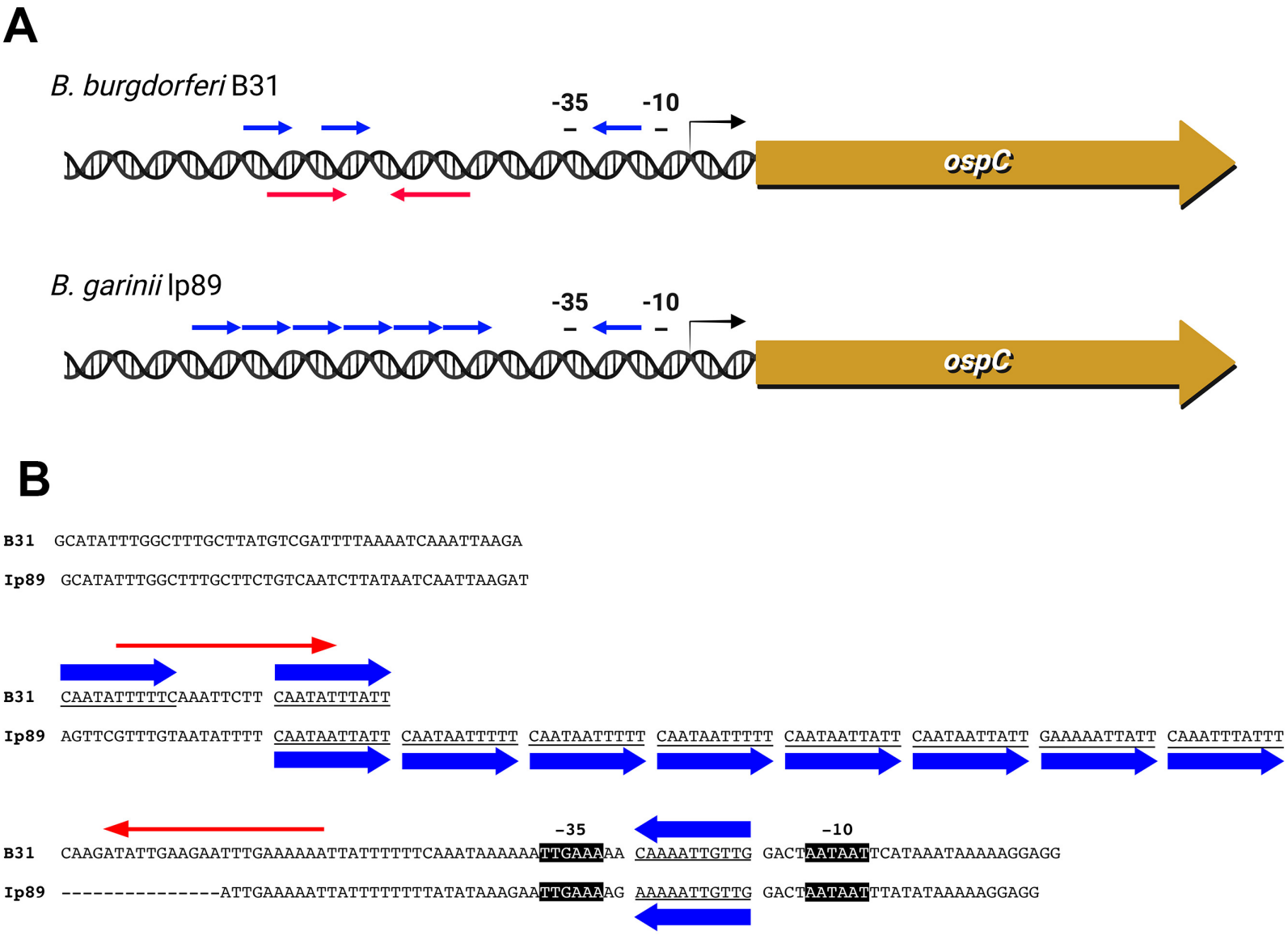
A
B. burgdorferi B31
-35
-10
ospC
B. garinii lp89
-35
-10
ospC
B
B31 GCATATTTGGCTTTGCTTATGTCGATTTTAAAATCAAATTAAGA
Ip89 GCATATTTGGCTTTGCTTCTGTCAATCTTATAATCAATTAAGAT
B31 CAATATTTTTCAAATTCTT CAATATTTATT
Ip89 AGTTCGTTTGTAATATTTT CAATAATTATT CAATAATTTTT CAATAATTTTT CAATAATTTTT CAATAATTATT CAATAATTATT GAAAAATTATT CAAATTTATTT
-35
-10
B31 CAAGATATTGAAGAATTTGAAAAAATTATTTTTTCAAATAAAAAATTGAAAAA CAAAATTGTTG GACTAATAATTCATAAATAAAAAGGAGG
Ip89 ----------ATTGAAAAATTATTTTTTTTATATAAAGAATTGAAAAG AAAAATTGTTG GACTAATAATTTATATAAAAAGGAGG

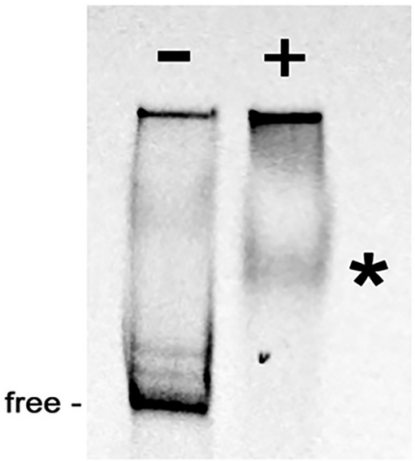

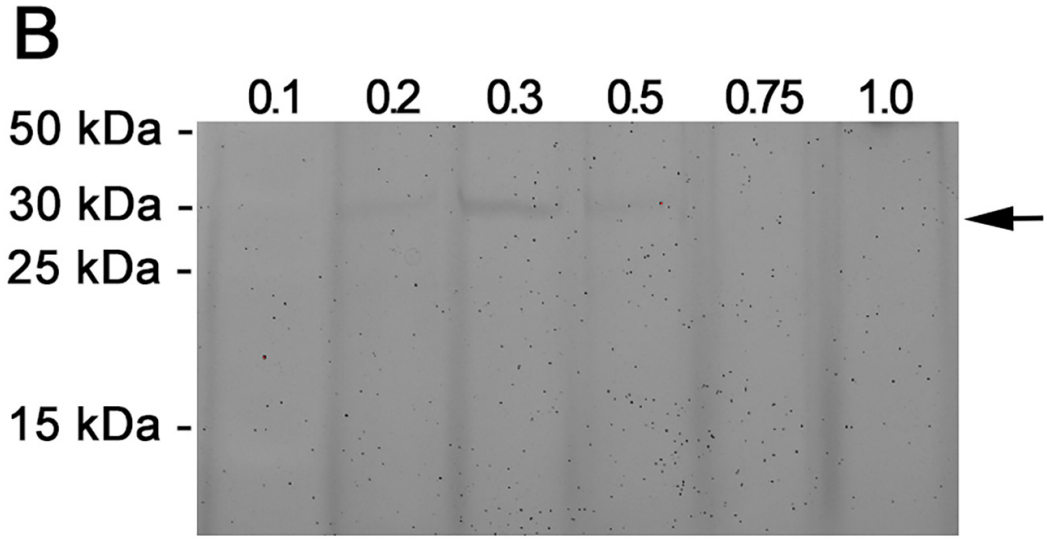

C

MAVGENKEQILNVRIEDEIKTSYLNYAMSVIVSRALPDVRDGLKPVHRRILYSMYEMGLRSDKAFKKAGRIVGDVLGKYHPH

GDQSIYDALVRLAQDFSLRYPVIRGQGNFGSIDGDPPAAMRYTEAKMEKITEYIVKDIDKETVNFKSNYDDSLSEPEIMPSS

FPFLLVNGSSGIAVGMATNMAPHNLREICDAIVYMLDNENASIFDLLKIVKGPDFPTFGEIVYNDNLIKAYKTGKGSVVIRA

RYHIEERAEDRNAIIVTEIPYTVNKSALLMKVALLAKEEKLEGLLDIRDESDREGIRIVLEVKRGFDPHVIMNLLYEYTEFK

KHFSINNLALVNGIPKQLNLEELLFEFIEHRKNIIERRIEFDLRKAKEKAHVLEGLNIALNNIDEVIKIIKSSKLAKDARER

LVSNFGLSEIQANSVLDMRLQKLTALEIFKLEEELNILLSLIKDYEDILLNPVRIINIIREETINLGLKFGDERRTKIIYDE

EVLKTSMSDLMQKENIVVMLTKKGFLKRLSQNEYKLQGTGGKGLSSFDLNDGDEIVIALCVNTHDYLFMISNEGKLYLINAY

EIKDSSRASKGQNISELINLGDQEEILTIKNSKDLTDDAYLLLTTASGKIARFESTDFKAVKSRGVIVIKLNDKDFVTSAEI

VFKDEKVICLSKKGSAFIFNSRDVRLTNRGTQGVCGMKLKEGDLFVKVLSVKENPYLLIVSENGYGKRLNMSKISELKRGAT

GYTSYKKSDKKAGSVVDAIAVSEDDEILLVSKRSKALRTVAGKVSEQGKDARGIQVLFLDNDSLVSVSKFIK

D

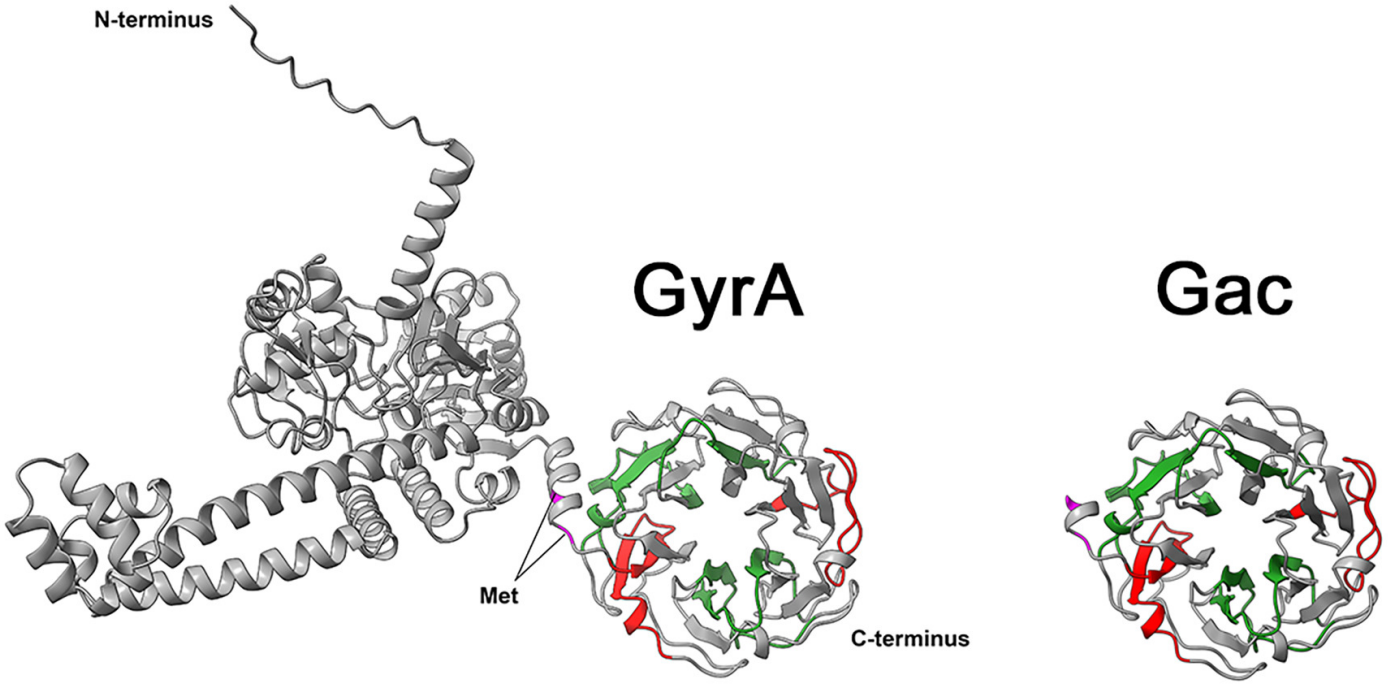

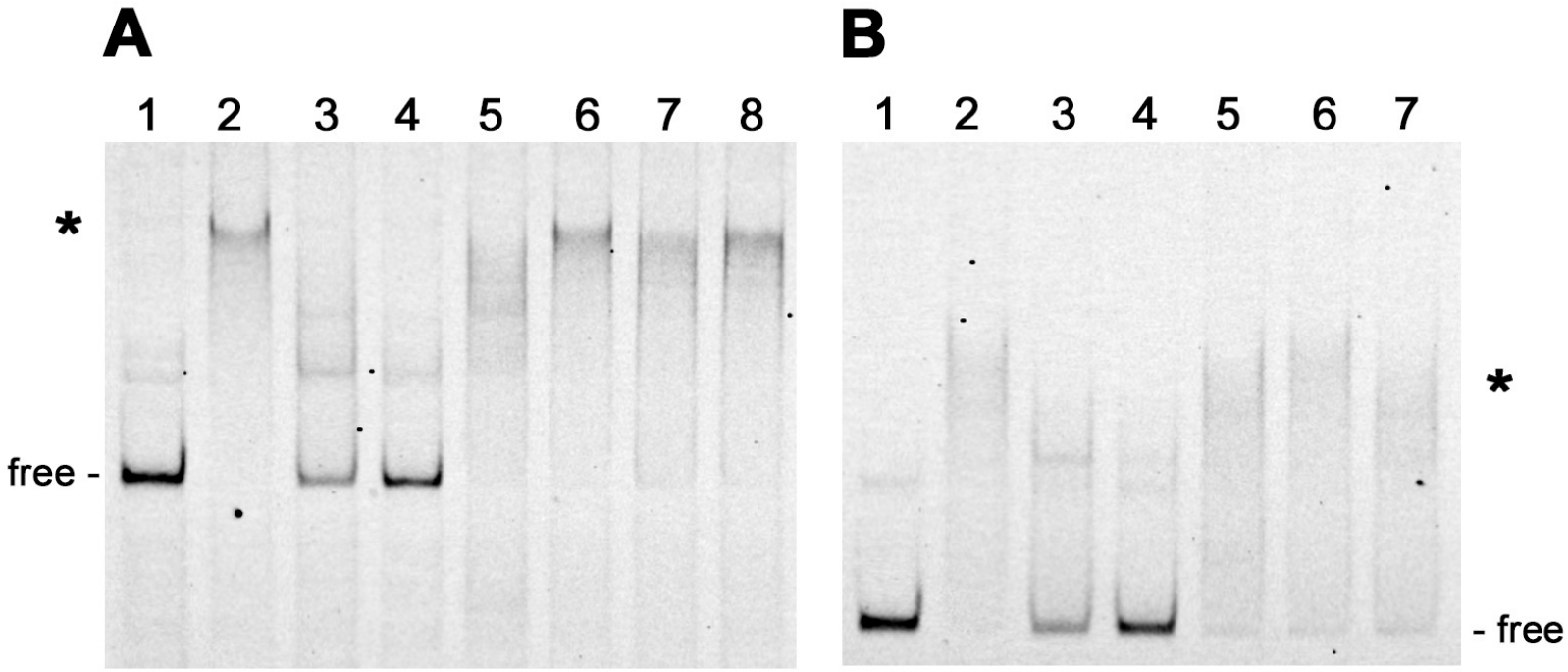
A
1 2 3 4 5 6 7 8
*
free -
B
1 2 3 4 5 6 7
*
- free

```
                                                                                                                                                                                                                                                                                                                                                                                                                                                                                                                                                                                                                                                                                                                                                                                                                                                                                                                                                                                                                                                                                                                                                                                                                                                                                                                                                                                                                                                                                                                                                                                                                                                                                                                                                                                                                                                                                                                                                                                                                                                                                                                                                                                                                                                                                                                                                                                                                                                                                                                                                                                                                                                                                                                                                                                                                                                                                                                                                                                                                                                                                                                                                                                                                                                                                                                                                                                                                                                                                                                                                                                                                                                                                                                                                                                                                                                                                                                                                                                                                                                                                                                                                                                                                                                                                                                                                                                                                                                                                                                                                                                                                                                                                                                                                                                                                                                                                                                                                                                                                                                                                                                                                                                                                                                                                                                                                                                                                                                                                                                                                                                                                                                                                                                                                                                                                                                                                                                                                                                                                                                                                                                                                                                                                                                                                                                                                                                                                                                                                                                                                                                                                                                                                                                                                                                                                                                                                                                                                                                                                                                                                                                                                                                                                                                                                                                                                
probe ..GCATATTTGGCTTTGCTTATGTCGATTTTAAAATCAAATTAAGACAATATTTTTCAAATTCTTCAATATTTATTCAAGATATTGAAGAATTTGAAAAAATTATTTTTTCAAATAAAAAATTGAAAAACAAAATTGTTGGACTAATAATTCATAAATAAAAAGGAGG..
Comp A  GCATATTTGGCTTTGCTTATGTCGATTTTAAAATCAAATTAAGACAATATTTTTCAAATT
Comp B                                AATCAAATTAAGACAATATTTTTCAAATTCTTCAATATTTATTCAAGATATTGAAGAAT
Comp C  GCATATTTGGCTTTGCTTATGTCGATTTTAAAATCAAATTAAGACAATATTTTTCAAATTCTTCAATATTTATTCAAGATATTGAAGAATTTGAAAAAATTATTTTTTCAAATAAAAAATTGAAAAACAAAATTGTTGGA
Comp D                                        ATTTTTCAAATTCTTCAATATTTATTCAAGATATTGAAGAATTTGAAAAAATTATTTTTTCAAATAAAAAATTGAAAAACAAAATTGTTGGACTAATAATTCATAAATAAAAAGGAGG
Comp E                                                  TTATTCAAGATATTGAAGAATTTGAAAAAATTATTTTTTCAAATAAAAAATTGAAAAACAAAATTGTTGGA
Comp F                                                                                TTGAAAAAATTATTTTTTCAAATAAAAAATTGAAAAACAAAATTGTTGGACTAATAATTCATAAATAAAAAGGAGG
Comp G                                                                                                  AATTGAAAAACAAAATTGTTGGACTAATAATTCATAAATAAAAAGGAGG
```

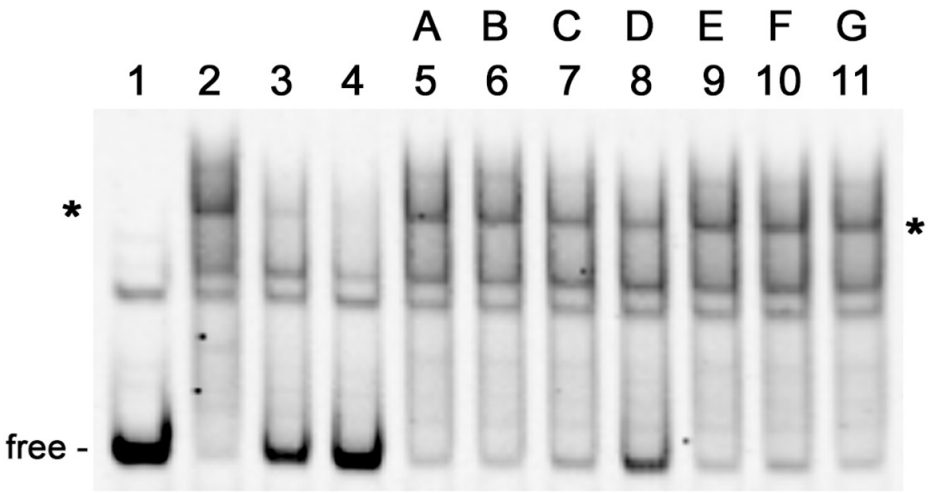

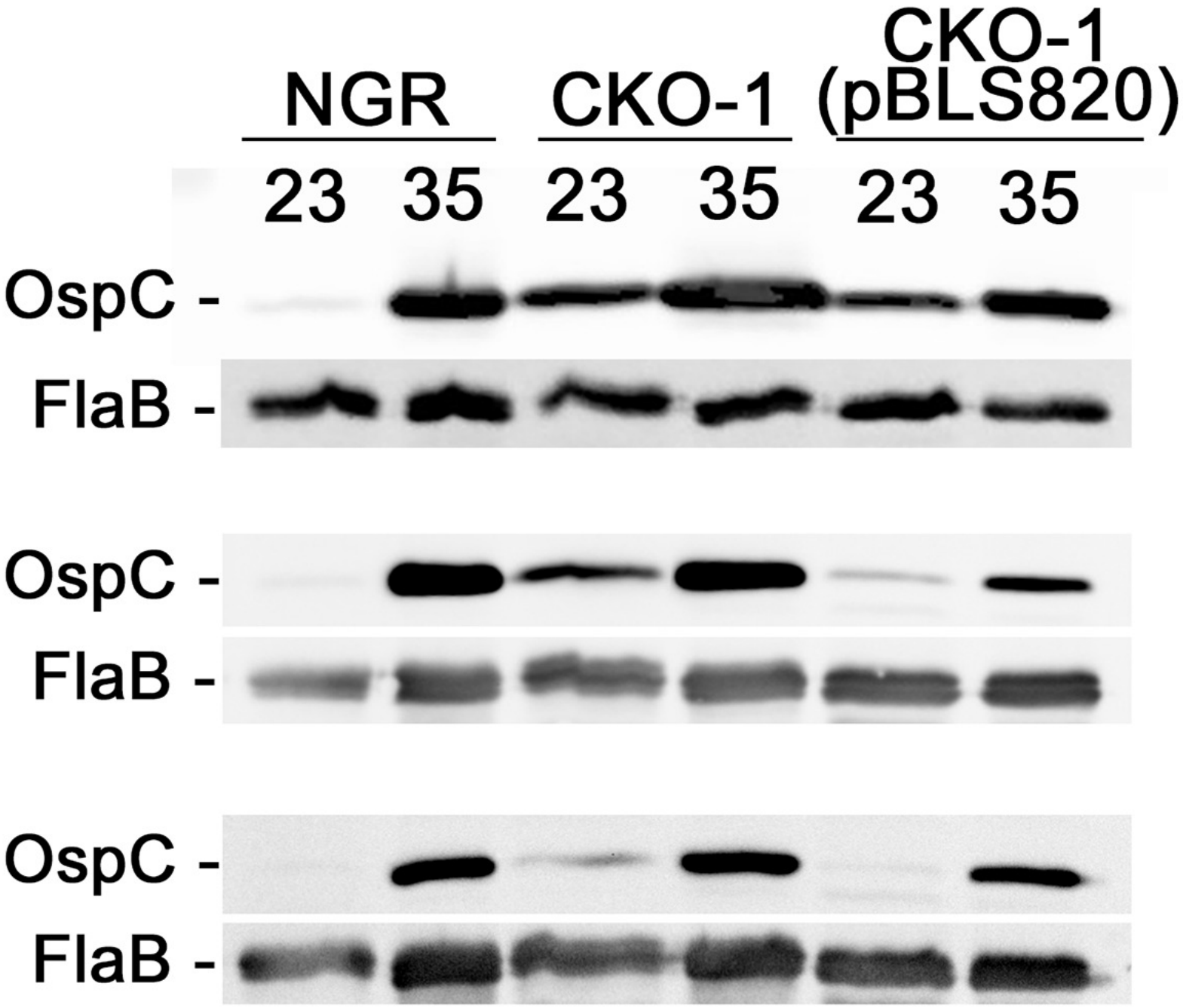
NGR
CKO-1
CKO-1 (pBLS820)
23
35
23
35
23
35
OspC -
FlaB -
OspC -
FlaB -
OspC -
FlaB -

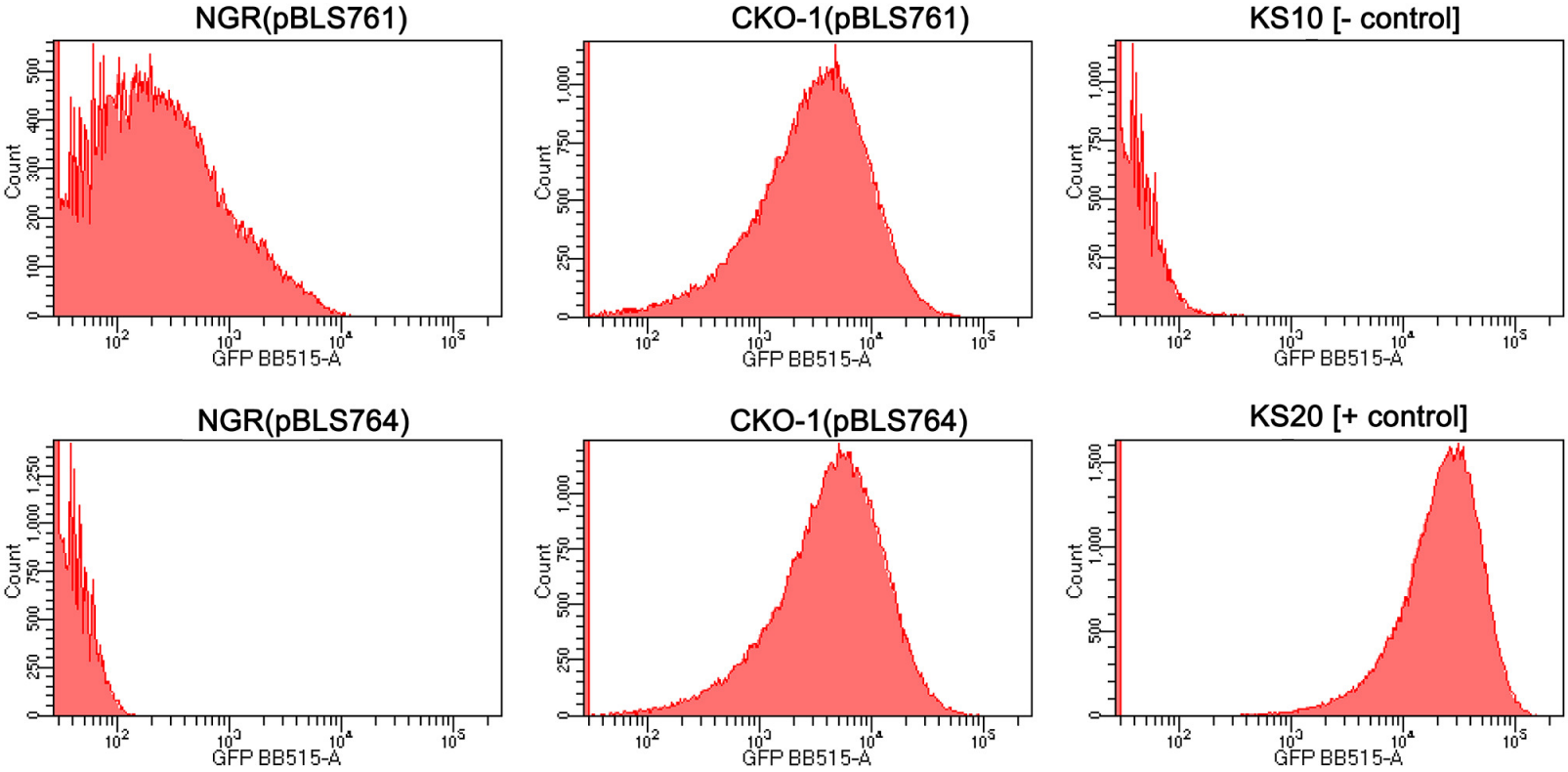
NGR(pBLS761)
CKO-1(pBLS761)
KS10 [- control]
NGR(pBLS764)
CKO-1(pBLS764)
KS20 [+ control]
Count
GFP BB515-A

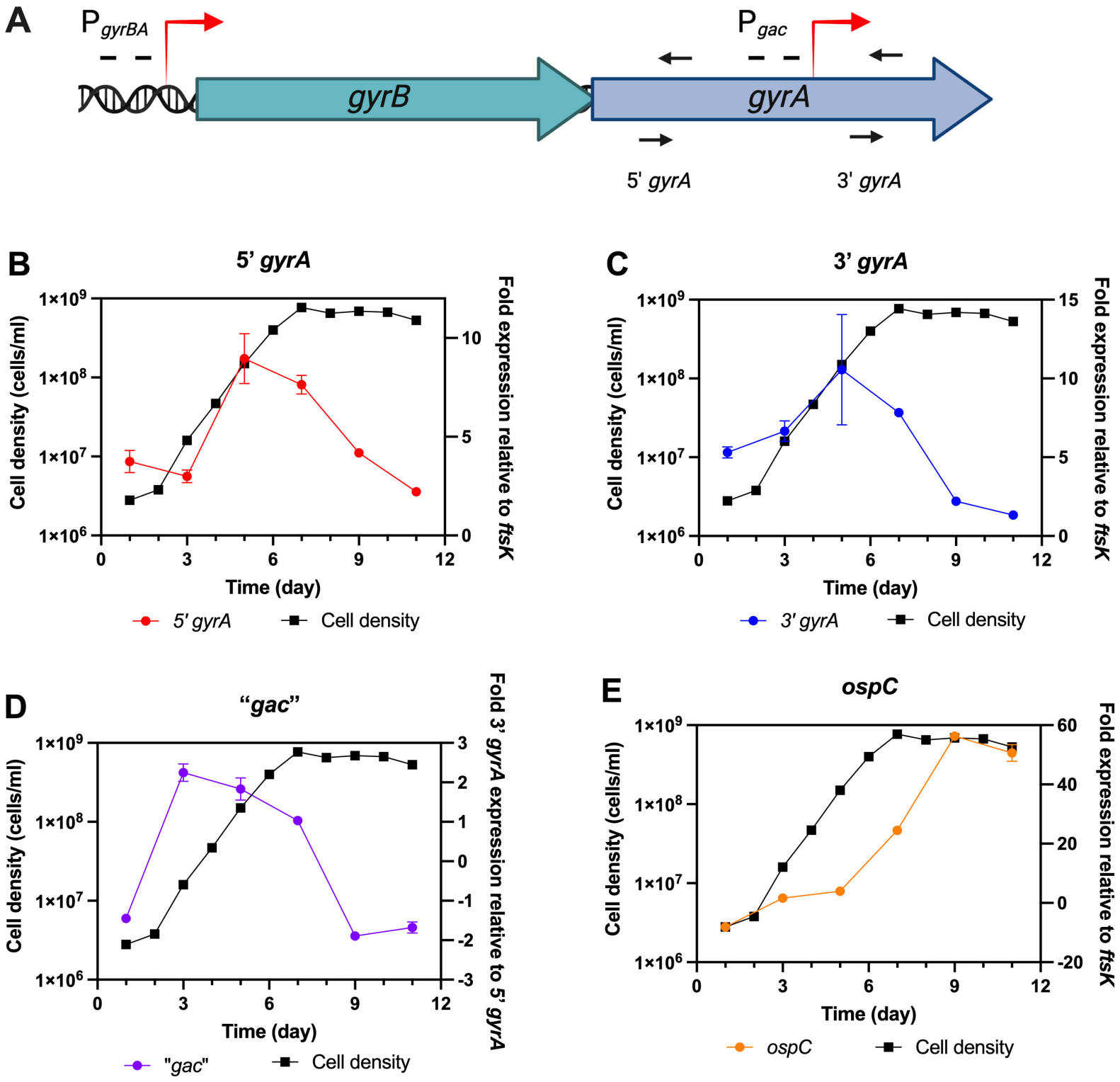
A
P gyrBA
P gac
gyrB
gyrA
5' gyrA
3' gyrA
B
5' gyrA
Cell density (cells/ml)
Fold expression relative to ftsK
Time (day)
5' gyrA
Cell density
C
3' gyrA
Cell density (cells/ml)
Fold expression relative to ftsK
Time (day)
3' gyrA
Cell density
D
"gac"
Cell density (cells/ml)
Fold 3' gyrA expression relative to 5' gyrA
Time (day)
"gac"
Cell density
E
ospC
Cell density (cells/ml)
Fold expression relative to ftsK
Time (day)
ospC
Cell density

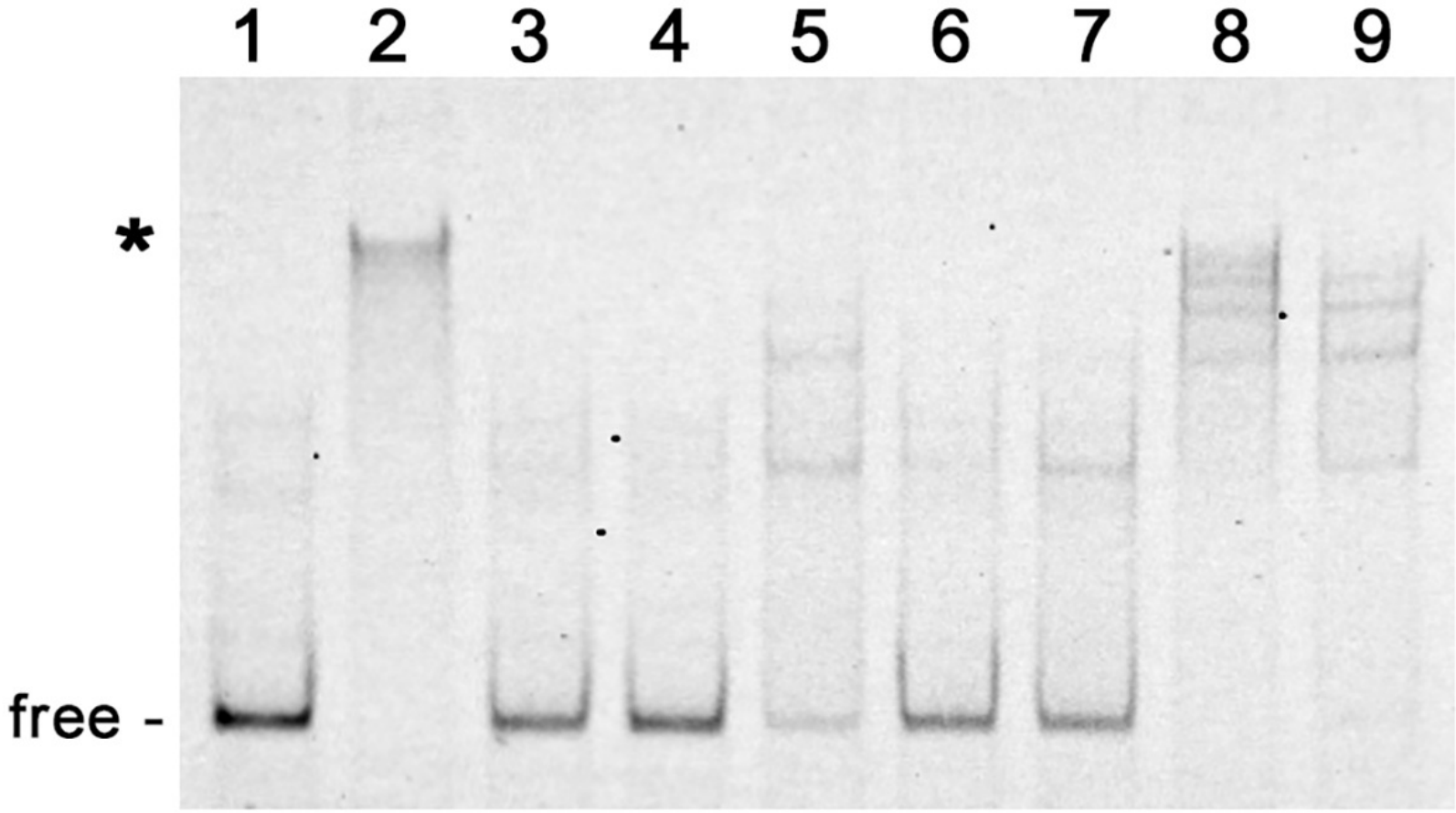
1
2
3
4
5
6
7
8
9
*
free -

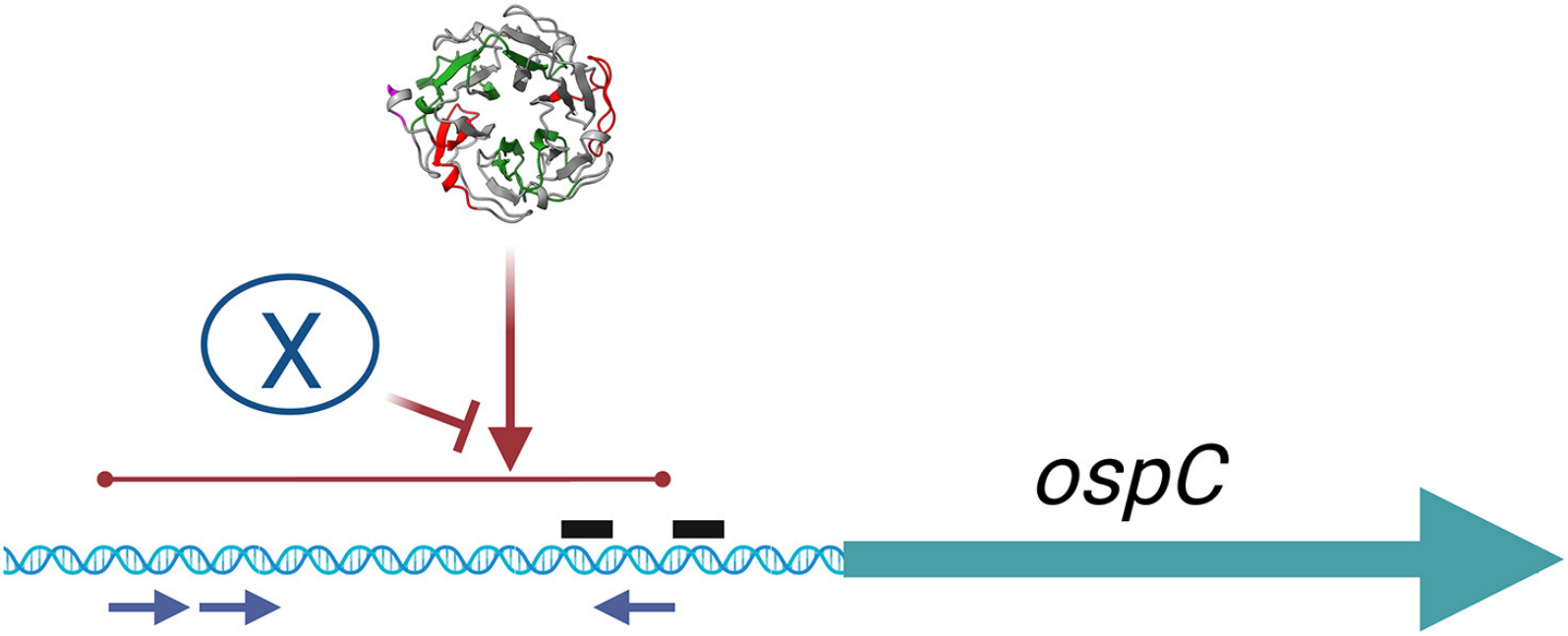
X
ospC

Gac is a transcriptional repressor of the Lyme disease spirochete's

OspC virulence-associated surface protein

by

Tatiana N. Castro-Padovani, Timothy C. Saylor, Olivia T. Husted, Andrew C. Krusenstjerna,

Nerina Jusufovic, and Brian Stevenson

Supplemental Tables and Figures

Supplemental Table S1. Sequences of synthetic DNAs and oligonucleotide primers used in this study

DNA name	Purpose	Sequence (5' to 3')
5.1	insert to produce pBLS761	GGTACCGCATATTTGGCTTTGCTTATGTCGATTTTAAAATCAAAT TAAGACAATATTTTTCAAATTCTTCAATATTTATTCAAGATATTGA AGAATTTGAAAAAATTATTTTTTCAAATAAAAAATTGAAAAACA AAATTGTTGGACTAATAATTCATAAATAAAAAGGAGGATCC
5.4	insert to produce pBLS764	GGTACCAATTGAAAAACAAAATTGTTGGACTAATAATTCATAAA TAAAAAGGAGGATCC
ospC 1010	PCR B31 *ospC* promoter/operator for production of pBLS760 and EMSA probe, competitors A, D, F, and G	ATATATGGATCCTCCTTTTTATTTATGAATTATTAG
ospC 1011	PCR B31 *ospC* promoter/operator to produce pBLS756	ATATATGGTACCGCATATTTGGCTTTGCTTATG
ospC 1021	PCR Ip89 *ospC* promoter/operator to produce pBLS756	ATATATGGTACCGCATATTTGGCTTTGCTTCTG
ospC 1021	PCR Ip89 *ospC* promoter/operator for DNA affinity and EMSA probes	ATATATGGATCCTCCTTTTTATATAAATTATTAG
flaB F	Annealed to *flaB* R to form *flaB* Competitor	AACAGGCAAAAGGATTTGCCAAAGTCAGAAATT
flaB R	Annealed to *flaB* F to form *flaB* Competitor	AATTTCTGACTTTGGCAAATCCTTTTGCCTGTT
ospAB F	Annealed to *ospAB* R to form *ospAB* Competitor	GTATTAAGTTATATTAATATAAAAGGAGAATATATT
ospAB R	Annealed to *ospAB* F to form *ospAB* Competitor	AATATATTCTCCTTTTATATTAATATAACTTAATAC

CompB1F	Annealed to CompB1R to form competitor A	GCATATTTGGCTTTGCTTATGTCGATTTTAAAATCAAATTAAGAC AATATTTTTCAAATT
CompB1R	Annealed to CompB1F to form competitor A	TTAAACTTTTTATAACAGAATTAAACTAAAATTTTAGCTGTATTC GTTTCGGTTTATACG
CompB2F	Annealed to CompB2R to form competitor B	AATCAAATTAAGACAATATTTTTCAAATTCTTCAATATTTATTCAA GATATTGAAGAAT
CompB2R	Annealed to CompB2F to form competitor B	TAAGAAGTTATAGAACTTATTTATAACTTCTTAAACTTTTTATAAC AGAATTAAACTAA
761 AF	PCR *ospC* competitor C	GCATATTTGGCTTTGCTTATG
761 DF2	PCR *ospC* competitor E	TTATTCAAGATATTGAAGAATTTGAAA
761 ER3	PCR *ospC* competitors C and E	TCCAACAATTTTGTTTTTCAA
M13 Forward	PCR *ospC* and lp17 telomere probes and competitors	GTAAAACGACGGCCAG
M13 Reverse	PCR *ospC* and lp17 telomere probes and competitors	CAGGAAACAGCTATGAC
TL16g	PCR lp17 telomere region, for cloning	AGACTAATAAAATAATGAATA
TL16h	PCR lp17 telomere region, for cloning	GTATTTTGACTCAAAACTTTA
gyrA-F	Q-RT-PCR of *gyrA* 5’ end	GTAGCCATTCCAACAGCAATTC
gyrA-R	Q-RT-PCR of *gyrA* 5’ end	CGATTCTTTAAGTGAGCCTGAGA
gac-F	Q-RT-PCR of *gyrA* 3’ end	CTTACAACTGCAAGTGGAAAGATAG

gac-R	Q-RT-PCR of *gyrA* 3’ end	ACAATAACACCTCGTGACTTTACT
ospC-F	Q-RT-PCR of *ospC*	TGAAGCGTTGCTGTCATCTAT
ospC-R	Q-RT-PCR of *ospC*	GCATAAGCTCCCGCTAACA
ftsK-F	Q-RT-PCR of *ftsK*	GACCTTCTGATGAGCCAATGT
ftsK-R	Q-RT-PCR of *ftsK*	GCTGCTCTGTTGTAACCTATCT

Supplemental Table S2. Relative changes in OspC protein levels in analyses of *B. burgdorferi* NGR, CKO-1, and CKO-1 (pBLS820), as shown in Figure 5. The immunoblots were imaged with a ChemiDoc MP (Bio-Rad, CA), and densities analyzed with background compensation using Image-Lab software (Bio-Rad). **A.** relative differences between strains at the same temperature. For example, in western 1, CKO-1 produced 23x more OspC than did NGR at 23°C. **B.** relative changes of the same strain at 23°C vs. 35°C. For example, in western 1, NGR produced 32x more OspC after shift to 34°C.

A.

Western	Strain	Temperature	
		23°C	35°C
1	CKO-1 vs NGR	23	1.4
	CKO-1 (pBLS820) vs NGR	14	1.1
	CKO-1 vs CKO-1 (pBLS820)	1.6	1.2
2	CKO-1 vs NGR	17	0.92
	CKO-1 (pBLS820) vs NGR	2.5	0.22
	CKO-1 vs CKO-1 (pBLS820)	6.9	4.3
3	CKO-1 vs NGR	6.4	1.1
	CKO-1 (pBLS820) vs NGR	1.5	0.69
	CKO-1 vs CKO-1 (pBLS820)	4.2	1.2

B.

Western	Strain	Change when Shifted from 23°C to 35°C
1	NGR	32
	CKO-1	2.0
	CKO-1 (pBLS820)	2.6
2	NGR	72
	CKO-1	3.9
	CKO-1 (pBLS820)	6.2
3	NGR	57
	CKO-1	10
	CKO-1 (pBLS820)	26

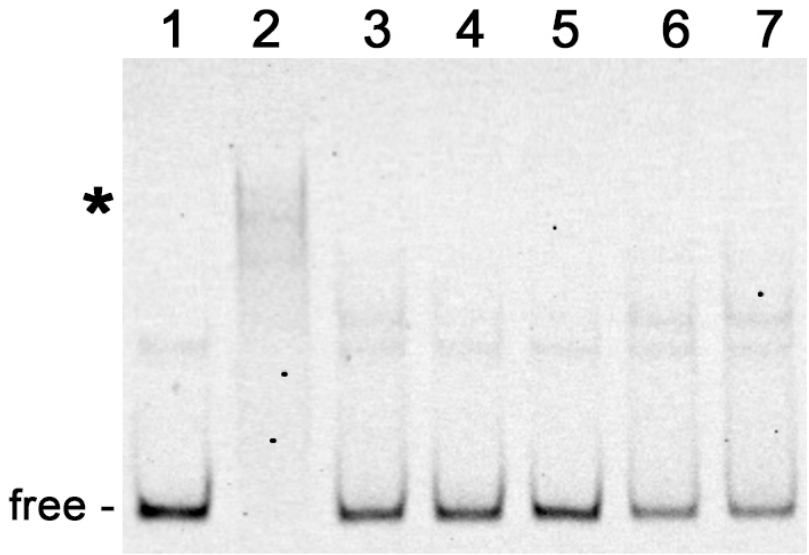

Supplemental Figure S1. Representative EMSA of purified recombinant Gac with labeled B31 *ospC* operator/promoter DNA and unlabeled competitors. Shifted DNAs are indicated with asterisks. Unoccupied DNAs are labeled "free". Labeled B31 operator/promoter (10 nM) without (lane 1) and with 25 nM Gac (lanes 2-7). Lane 2: no added competitor. Lane 3: plus 10x excess unlabeled B31 *ospC* operator/promoter. Lane 4: plus 25x excess unlabeled B31 *ospC* operator/promoter. Lane 5: plus 25x unlabeled pCR2.1 amplicon. Lane 6: plus 25x excess unlabeled *flaB* DNA. Lane 7: plus 25x unlabeled *ospAB* DNA.

-35 -10

CCAGTAAGGATTATTAATATTATAAGAGAAGAAACTATTAATTTAGGTTTGAAATTTGGCGATGAACGTCGAACTAAAATAATTTATGATG

RBS Met Met

AGGAGGTTTTAAAAACTAGTATGTCGGATTTAATGCAAAAAGAAAATATTGTTGTTATGCTTACAAAGAAAGGTTTCCTTAAAAGACTT
TCACAAAATGAGTATAAATTGCAAGGTACGGGAGGAAAAGGACTAAGTTCGTTTGATCTAAATGATGGAGATGAGATTGTTATTGCTTT
GTGTGTCAATACTCATGATTATTTATTTATGATTTCAAATGAAGGAAAGCTTTATTTAATCAATGCTTATGAAATAAAAGATTCTTCAAGAG
CTTCAAAAGGTCAGAATATTAGTGAGCTTATTAATTTAGGAGATCAAGAAGAAATATTAACTATTAAGAATAGTAAAGATTTAACTGATG
ATGCTTATTTATTGCTTACAACTGCAAGTGGAAAGATAGCTAGATTCGAATCTACAGATTTTAAAGCAGTAAAGTCACGAGGTGTTATTG
TTATTAAACTGAATGATAAAGATTTTGTTACAAGTGCAGAGATTGTTTTTAAGGATGAAAAAGTAATTTGTCTTTCTAAAAAGGGTAGTG
CATTTATATTTAATTCAAGGGATGTTAGGCTTACTAATAGAGGTACCCAAGGTGTTTGTGGAATGAAATTAAAAGAAGGTGATTTGTTTG
TTAAAGTTTTATCGGTTAAAGAAAATCCTTATCTTTTGATTGTTTCTGAAAATGGGTATGGAAAAAGGTTAAACATGTCTAAAATATCTG
AGCTTAAAAGAGGAGCCACTGGTTATACTAGTTATAAAAAATCTGATAAAAAAGCGGGTAGTGTTGTTGATGCTATAGCAGTTTCAGAG
GATGATGAAATCTTGCTTGTAAGTAAACGTTCAAAAGCTTTAAGAACAGTAGCTGGAAAAGTATCTGAACAAGGCAAAGATGCTAGAG
GAATTCAAGTATTATTTCTTGATAATGACAGCTTGGTTTCTGTTTCAAAATTTATTAAATAA

Stop

Supplemental Figure S2. Sequence of the insert of pBLS820 that encodes Gac protein. Putative -10 and -35 promoter elements and the ribosome binding site (RBS) are indicated in **purple**. The *gac* ORF is preceded by two in-frame methionine codons, indicated in **green**. The *gac* termination codon is indicated in **red**.